CAES Future Scenarios:

An Investment Analysis for Denmark

Prepared by:

Georges Salgi

Submitted on:

19 January 2006

Aalborg University

Energy Planning, 10th semester

Theme:	Masters Thesis
Title:	CAES Future Scenarios: An Investment Analysis for Denmark
Period:	Spetember 2005 – January 2006
Prepared by:	Georges Salgi
Supervisor:	Henrik Lund
Number of Copies:	3
Number of Pages:	67

Abstract

The increase of the renewable energy share in the Danish electricity system increases the need for flexible technologies that can maintain the electricity balance. Energy storage is one possible solution to this problem. On a utility scale, CAES is one of the technologies with a great feasibility potential compared to other storage technologies. The operation of CAES requires high volatility in electricity prices. The large hydro capacities in the Nordic region however have so far kept the prices from fluctuating enough to allow for CAES investments. This report studies the effect of technological development and possible future prices development on the feasibility of CAES plant investments of various capacities. It is found that advanced high efficiency CAES plants can become feasible as early as the year 2012.

Preface

This report is the final thesis for the Masters Degree in Energy Planning at the department of Development and Panning, Aalborg University. The thesis constitutes the fourth major project done during this masters program.

Work on the thesis started on the 01st of September 2005. During the initial phase, a thorough literature review was conducted with the purpose of identifying the proper research question and approach. The second was used to dive into the CAES components technology in order to determine the appropriate model for each. This lead to the third phase of developing the technical model and testing it to confirm with data from literature. The fourth phase constituted an attempt to find the optimal CAES operational strategy on the market and model it. Once this was established, the model was further calibrated and tested before the main results were calculated. The time span allocated has not allowed for the desired simulations and detail level in the results and the report. It is hoped that the developed model can be used later though to carry on this task.

I find myself indebted to thank all those who supported me and helped me throughout the project. Special thanks to my supervisor Henrik Lund for his time, valuable suggestions, and helpful attitude. Many thanks also to Bernd Möller from the Energy Planning Research Group at Aalborg University for his enthusiasm and help. Thanks to Brian Elmegaard from DTU for his collaboration with discussions and literature material. Also thanks to Peter Børre Erriksen, Bjarne Donslund, and Jens Pedersen from Energinet.dk for their valuable time and support. The working environment at the office has been a great pleasure thanks to Brian Vad Mathiesen, Decharut Sukkumnoed, and Morten Boje Blarke. Finally, special thanks to my friends Adela, Bram, Ihab, and Lee who were there for me and provided me with a place to stay during the last period.

Aalborg, 19 January 2006

_____
Georges Salgi

TABLE OF CONTENT

List of Symbols

AIC: Annual Investment Cost

AT: Advanced Technology

CAES: Compressed Air Energy Storage

CDT: Current Day Technology

CHP: Combined Heat and Power

DKK: Danish Krone

ELR: Electricity Ratio

FAC: Fixed Annual Cost

FR: Fuel Ratio

GE: General Electric

GT: Gas Turbine

HR: Heat Ratio

IPLE: "Investering og prisdannelse på et liberaliseret elmarked" report.

NAP: Net Annual Profit

NOK: Norwegian Krone

NPV: Net Present Value

SOAT: State of the Art Technology

VAOI: Variable Annual Operational Income

η_{GT}: Gas Turbine Cycle Efficiency

List of Figures

List of Tables

1. Introduction

The benefits of utilizing renewable energy sources such as wind and solar energy are numerous from an environmental and socio-economic perspective. Besides offering an emission free alternative to the polluting fossil fuel combustion, renewable sources enhance the energy independence of the national economy as it depends less on foreign and usually unstable fossil fuel sources. The success of the Danish wind turbine industry has also shown that economic benefits through employment and export can be gained from the development of such technologies.

While the investment costs for most renewable technologies remain high, some technologies such as wind turbines have reached a cost level where they can compete with the traditional fossil fuel alternatives. Despite this fact, utility scale renewable energy contribution continues to face a major barrier hindering its expansion. The intermittent nature of solar insolation, wind, and waves make them unreliable energy sources as the power is not always produced when it is needed.

In Western Denmark, wind energy provided 32% of the electricity consumption in 2004. The current total installed capacity is 2400 MW, 160 MW being offshore. This compares to an electricity consumption that varies between 1,150MW and 3,800MW. It can be seen that with high wind velocities, the wind production can exceed the local electricity demand. Besides, the changing wind velocity gives rise to a large need of fast reserve capacity to regulate the power imbalances. The ability of the electricity system to absorb accommodate this high level of wind energy is further complicated by the high percentage of decentralized small scale CHP power plants whose production depends on the weather conditions.

The system operator in Western Denmark (Energinet.dk) has been so far able to deal with these challenges by using both local thermal resources and connections to neighboring electricity systems. Major CHP plants are gradually starting to operate on market conditions which is expected to improve the power balance. As neighboring countries have plans to increase their wind production in the future years though, this could reduce the regulating capacities available from abroad. From a socio-economic

and security of supply perspective, local reserves are preferred, especially that exported electricity from wind power is sold at low prices and bought again later at higher prices.

Electricity storage is one of the possible solutions to the above mentioned challenges. Very few technologies tend to be economic at a utility scale however. On a local level in Denmark, one of the potentially feasible technologies available nowadays is *compressed air energy storage* (CAES). CAES is a modification of the basic gas turbine (GT) technology, where low cost electricity is used to store compressed air in an underground cavern. This air is then expanded in a gas turbine to produce electricity during peak demand hours (Figure 1.1). As it is a derived from GT technology, CAES technology is readily available and reliable. Two plants have been constructed in the world so far in Germany and the USA of 390 MW and 110 MW turbine capacities respectively.
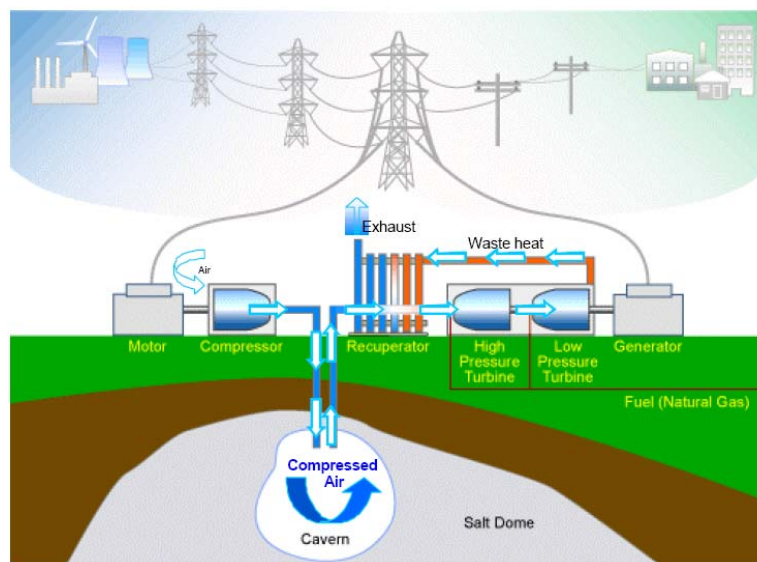
Figure 1.1: Basic CAES plant operation: air is compressed and stored in an underground cavern before being expanded in a gas turbine. (LCRA, 2003)

In order to operate profitably in a liberalized market, a CAES facility depends on several factors relating mainly to electricity and natural gas prices. This has been a reason why the majority of the proposed CAES projected over the world never materialized. In system with hydro power, pumped hydro storage provides a much cheaper alternative than CAES. As the Danish system is closely connected to the hydro dominated Nordic power system, this can cause a challenge to implementing CAES in Denmark despite its benefits from a socio-economic perspective.

In the future though, electricity demand is projected to increase. Coupled with plans to increase wind energy capacities in the Nordic countries and Northern Germany, this can lead to changing conditions where improved CAES technologies can become profitable to operate in Denmark.

This project takes its point of departure in the above discussion and attempts to answer the following research question:

"What are the possible future favorable conditions that could encourage a private investment in a CAES plant in Denmark?"

In order to answer the main question, two main sub-questions need to be addressed:
1- What are the possible future technology developments in the CAES technology?
2- What are the possible future scenarios for the Danish electricity system?

Chapter 2 (Methodology) describes the main approach used to answer the above questions and gives an overview of the report structure.

2.   Methodology

This chapter gives an overview of the main methodology applied to answer the research question along with the major assumptions taken. Section 2.1 gives an overview of the CAES model which is the main analysis tool used to perform future simulations. Section 2.2 then defines the framework used to answer the sub-questions mention in Chapter 1 regarding future technology and electricity system scenarios. Section 2.3 states some of the main underlying assumptions used in the study, and finally section 2.4 gives an overview of the report structure.

2.1   Analysis tool: the CAES plant model

The main objective of the report is to examine potential business opportunity for a CAES plant operating in Denmark. As in any future analysis, the uncertainty levels are relatively high regarding both the technology itself and its surrounding environment. Therefore, the analysis is regarded more as a mental exercise to try to answer "what if" questions about the future. Through varying the different affecting factors, the significance of each factor can be determined, and the risk that factor's variation can be assessed.

For this reason, a computer model that describes the plant technology and its operating environment was a part of the study performed. The first modeling part was thus to simulate the thermodynamic behavior of individual CAES plant components. These components are later used as building blocks to assemble a certain plant design and predict its performance.

The second modeling part was to predict the economic operational opportunities available for the plant. One of the major assumptions made is the use of a **deterministic price series** model where electricity prices are known over the period considered. In reality, operating an energy storage facility is more challenging as no exact knowledge is available regarding future prices. Taking a closer look at the electricity price series though, one can detect seasonal, weekly, and daily trends that tend to follow the electricity demand. A deterministic price model in a way assumes the plant operator has

accumulated enough experience about price fluctuation projections to take the right decision at the right time. The time span of the future price prediction required in real life is dependant on the storage size and the available plant capacity.

Using a deterministic price series allows for the simulation of various market opportunities (spot market, regulating market, etc.) by altering the time series considered. Here again, real life necessitates that the plant operator to be able to predict the proper market to bid on. The main source of regulating power need in Western Denmark is due to wind power. With wind prediction and other market tools available, the operator can be able to take a better judgment concerning the proper market to bid on and the best storage content to approach the specified period with. The exact method used to find the optimum operational strategy is described in detail in section 4.3.

2.2   Future Technology and Electricity System Scenarios

Three main technological scenarios are utilized in the analysis. The first scenario is based on the information available from the Alabama plant in the USA as it recently built (1991) and has higher efficiencies than the Huntorf plant in Germany. This technology is labeled "*Current Day Technology (CDT)*" and is used as the base scenario.

The *"State of the Art Technology (SOAT)"* scenario is derived from the CD scenario, the only difference being the turbine firing temperature which was inspired from the General Electric (GE) H system GT with reported combined cycle efficiencies exceeding 60% (Matta et al., 2004).

Finally, the *"Advanced Technology (AT)"* scenario is based on the assumption that the waste heat during compression can be saved and later utilized to save fuel in the expansion phase. The difference between the SOAT and the AT is an improved regenerator performance and the utilization of 50% the heat wasted during compression for fuel saving during expansion.

The main future electricity scenario is inspired from a recent study on the potential price development and future investment in the electricity market published by Risø Research

Center. The study is titled "Investering og prisdannelse på et liberaliseret elmarked" and can be downloaded free of charge from Risø website: www.risoe.dk. (Morthorst et al., 2005) For simplicity, the aforementioned report would be referred to as the IPLE report henceforth.

Before proceeding, it is important to stress that the values inspired from the IPLE report are not regarded as future projections but rather as a possible future scenario. Being a future analysis itself, the IPLE is based on numerous future assumptions which must be taken into consideration when interpreting the results. For example, a major assumption behind price projections is the so called "worse case" scenario which assumes *no further investment in the electricity sector apart from the already declared plans in the Nordic region.* Other assumptions include electricity and heat demand development, fuel prices, and CO_2 quota prices. These values are taken from the Danish Energy authority projections in the IPLE and are used the same in this report for consistency.

Besides, the future price variation in the IPLE report was found using the Balmorel model. The use of any model has a certain limitation to the level it can depict reality and the output varies depending on the targeted issue emphasized inthe model. For example, the Balmorel results depict the general price variation trends quit good. However, extreme price peaks and troughs are difficult to predict, as they could be the result of market imperfections such as the exercise of market power. Besides, the use of demand elasticity is employed in the model to find a balance in cases with production shortage, wheras the real market has so far shown very little demand elasticity. These facts need to be considered when interpreting the CAES simulation results, especially that energy storage technologies are designed to operate on the extremes of price variation. The reader is encouraged to refer to the IPLE report for a detailed description of the simulated price variation and their interpretation.

As the exact price time series is not available from the IPLE study, a modified version of the system prices of Western Denmark for the year 2002 was used instead. The first half of the year 2002 witnessed moderate prices that display the major trends with minimal extreme peaks and troughs. The other half of that year though was characterized by higher peeks as the water content in the hydro reserviours was low. The first half of

the year 2002 is thus taken and "mirrorred" over its half. This time series has been used in a previous study done at Aalborg University, and further description can be found in (Lund et al., 2004).

It is found that multiplying the normalized 2002 price series with the average annual prices results in price series with reasonable similarity to prices reported in the IPLE report. Figure 2.1 shows the average market price variation up to 2020 for a normal year in terms of weather and rainfall. Figure 2.2 shows the hourly price fluctuation between 2010 and 2020 for the 2002 series. Note that the IPLE results are in Norwegian Krone (NOK). The current rate of exchange is around 0.92 NOK per 1 DKK. For simplicity, it is assumed that the future rate of exchange is 1 NOK per DKK so that prices calculated are in DKK.
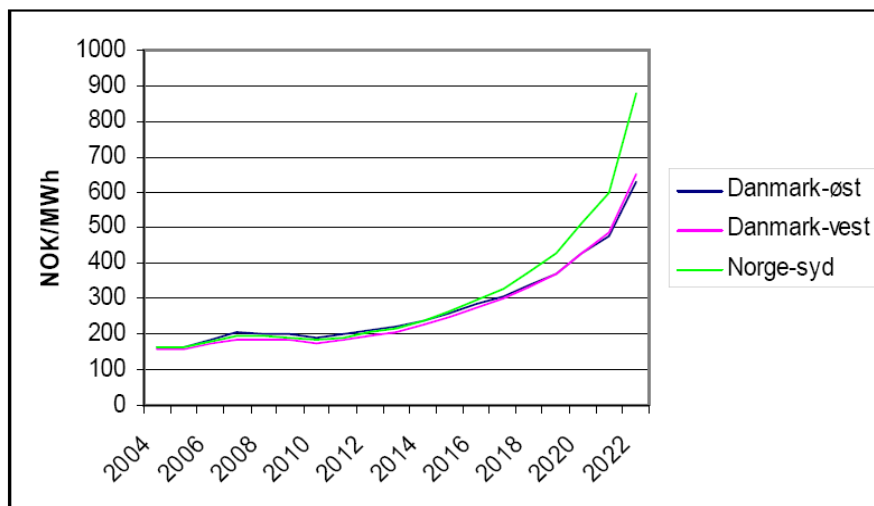
Figure 2.1: Average annual electricity price values from the IPLE report. (Morthorst et al., 2005)
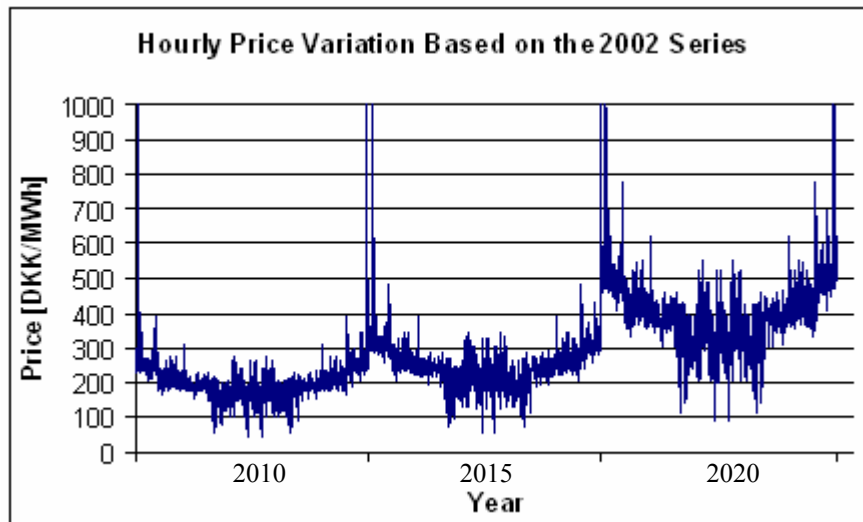
Figure 2.2: Hourly price variation for the years 2010, 2015, and 2020 based on the normalized 2002 prices time series multiplied by the average annual price.

Figures 2.3 and 2.4 show the duration curve for the modified 2002 time series and the IPLE curve for eastern Denmark. It can be seen that the overall price behavior in both is quite similar. This is confirmed in Table 2.1 where a summary of price values is given for the 2002 time series compared to predictions for East and West Denmark. Following the IPLE report, plans were announced to construct of an electrical connection between East and West Denmark, and this is expected to get the two areas closer in terms of price variation.

Total hours above %	2010		2015			2020		
	2002 Series	DK Ø	2002 Series	DK Ø	DK V	2002 Series	DK Ø	DK V
100	99	100	100	100	100	100	100	100
200	43	36	85	95	88	99	100	100
300	1	1	16	12	11	92	100	99
400	0	0	1	<1	<1	43	60	60
500	0	0	0	<1	0	10	6	8
600	0	0	0	<1	0	1	2	1

Table 2.1: Comparison of the variation of the 2002 modified time series compared to values from the IPLE report for east and west Denmark for the years 2010, 2015, and 2020.
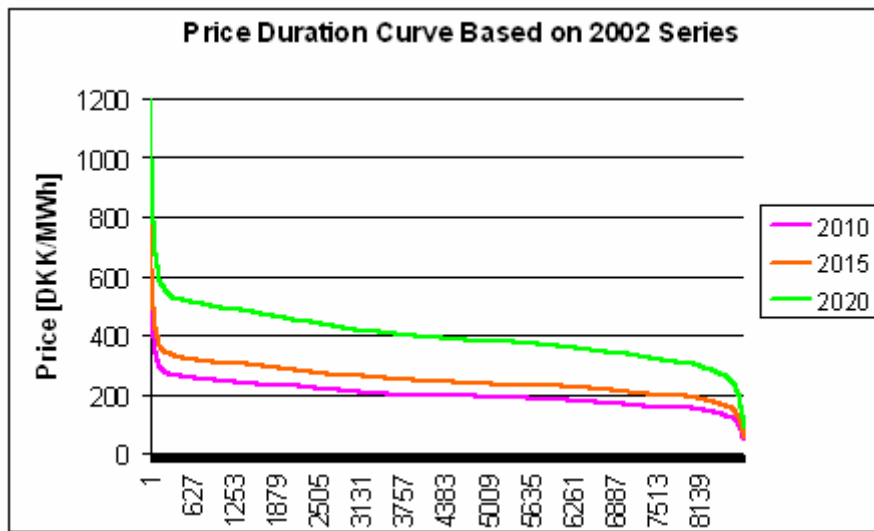
Figure 2.3: Duration curve for the prices shown in Figure 2.2.
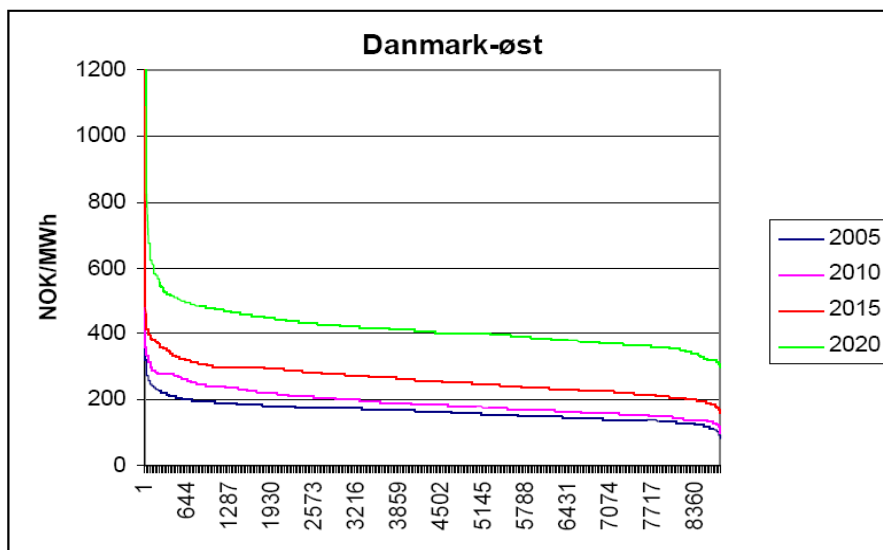
Figure 2.4: Duration curve for prices in East Denmark from the IPLE report. (Morthorst et al., 2005)

As an overall summary for the price time series, it is considered good enough to simply use the modified 2002 price time series to give a tentative time series for a "normal" weather year. Further modifications to the price time series are possible through the use of addition or multiplication factors.

2.3   Main Assumptions

Apart from the simulation model and future scenario assumptions, several other assumptions are made for the analysis, the main ones of which are:

- The analysis is performed from a business economic perspective. The only **benefits and costs considered are the ones that are given an established monetary value**, such as CO_2. Other factors such as environmental impact, potential employment, and effect on the national economy are not treated.

- The analysis is made from the perspective of a **single private investor that does not own other production/consumption facilities in the system**. In case the investor owns other facilities, the overall effect of the investment on the other facilities has to be considered as well.

- The investor does not face competitor investors neither in CAES nor in any other electricity production/consumption technology. This assumption excludes for example the potential of a growth in hydrogen technology or heat pumps. The development of these alternatives or the investment in further power production plants constitutes a risk to the CAES plant profitability.

- The market is assumed to be free with no entry or other institutional barriers.

- The effect of taxes or potential subsidies is not considered in the analysis.

- The basic Net Present Value (NPV) method is used for feasibility calculation. More thorough economic and financial methods can be necessary to properly address the high risk environment in a liberalized electricity market.

2.4   Report Structure

The report assumes that the reader has prior knowledge of the Danish electricity system and the electricity market associated with it. For readers who would like to have more material on this issue, the websites of the system operator www.energinet.dk and Nord Pool market (Nord Pool) provide a good system description. Several publications also describe this topic including the IPLE report where a thorough market description is provided.

Chapter 3: Technology Background gives a technological overview of the CAES technology. This includes an introduction to gas turbine technology, followed by CAES description and sample existing plant configurations.

Chapter 4: Model Description describes the model used for performing the simulations along with its accompanying assumptions. Both the technical and the operational model are described in this chapter.

Chapter 5: Analysis presents the future analysis performed by establishing the technology and electricity system scenarios. Simulation results and feasibility analysis is then presented.

Chapter 6: Conclusion and Reflections finally summarizes the results of the project and provides some reflections on the attained results.

3.   Technology Background

The basic Compressed Air Technology (CAES) is a variation of the gas turbine (GT) technology. Therefore, Section 3.1 starts by giving an overview of the GT technology. Section 3.2 then describes the main modifications of CAES and the corresponding operational characteristics. Section 3.33 concludes by presenting sample technical configurations of implemented CAES plants.

3.1   Gas Turbine Technology

The basic open cycle gas turbine (GT) consists of 3 main stages: compression, combustion, and expansion (Figure 3.1a). In a typical unit, air at atmospheric conditions is compressed in an axial compressor where its pressure and temperature are raised. The air is then mixed with fuel in a combustion chamber where the temperature is further increased. Finally, work is extracted from the flowing air in the turbine, thus resulting in a pressure and temperature drop. Typically, around 2/3 of the work extracted by the turbine is used to drive the compressor, while the other part is available as a net shaft work output (Sonntag et al., 2003).
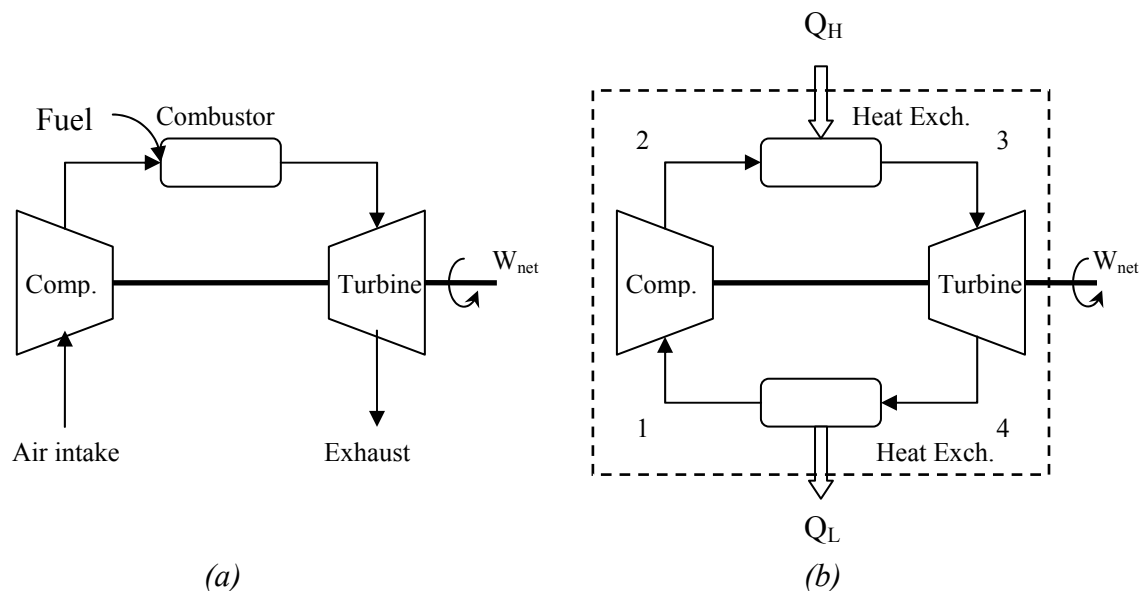
Figure 3.1: *(a) Simple open cycle gas turbine representation. (b) The standard air cycle representation of the simple cycle.*

Despite the fact that GTs operates on an open cycle where fresh fuel is added and the chemical composition of the working fluid is changed, a GT can be modeled as an *air-standard power cycle[1]* by replacing the combustion chamber by a heat exchanger and feeding the exhaust to the input after rejecting the extra heat content as shown in Figure 1b. The ideal air-standard power cycle representing a GT is known as the Brayton cycle or the *constant pressure cycle.* The Brayton cycle consists of 4 consecutive stages as shown on the P-*v* and the T-s diagrams of Figure 3.2:

- Isentropic compression (1 – 2)
- Isobaric heat absorption (2 – 3)
- Isentropic expansion (3 – 4)
- Isobaric heat rejection (4 – 5).
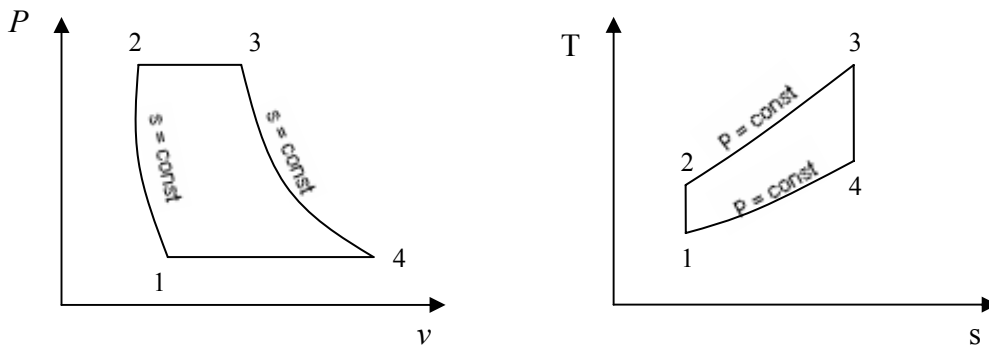
Figure 3.2: The P-v and T-s diagrams of a Brayton cycle. Note that the enclosed area represents the net work output from the cycle in both diagrams (Figure note to scale).

3.1.1   GT Efficiency

The GT heat engine cycle efficiency is defined as:

$$\eta_{GT} = \frac{Net\ work\ output}{Total\ heat\ input} = \frac{Q_H - Q_L}{Q_H} \quad \text{... 3.1}$$

[1] An air-standrad power cycle is a cycle where the mass of the air circulating is fixed such that there is no inlet or exhaust processes, the air is assumed to be ideal, all processes are internally reversible, and the combustion is replaced by heat transfer to an external source (Sonntag et al., 2003)

With the states labeled as in Figure 3.2, and assuming perfect gas behavior (ideal gas with constant specific heat), the Brayton cycle efficiency can be expressed as:

$$\eta_{GT,Brayton} = 1 - \frac{T_1}{T_2} = 1 - \frac{1}{Pr^{(k-1)/k}} \quad \text{.................................} \quad 3.2$$

Where:

- $\eta_{GT,Brayton}$ is the Brayton cycle efficiency
- Pr is the pressure ratio $Pr = \dfrac{P_2}{P_1}$
- k is the specific heat ratio, $k = \dfrac{C_p}{C_v}$

It can be deduced from equation 3.2 that increasing the pressure ratio results in improved cycle efficiency. The above expression however does not take into account the individual compressor and turbine efficiencies, which when included result in the following expression (Boyce, 2002):

$$\eta_{cycle,tc} = \left(\frac{n_t T_f - \dfrac{T_{amb} \, Pr^{\left(\frac{k-1}{k}\right)}}{\eta_c}}{T_f - T_{amb} - T_{amb}\left(\dfrac{Pr^{\left(\frac{k-1}{k}\right)}-1}{\eta_c} \right)} \right) \cdot \left(1 - \frac{1}{Pr^{\left(\frac{k-1}{k}\right)}} \right) \quad \text{..............} \quad 3.3$$

Where:

- η_c is the compressor isentropic efficiency,
- η_t is the turbine isentropic efficiency,
- T_{amb} is the ambient temperature (compressor inlet temperature),
- T_f is the firing temperature (turbine inlet temperature).

Equation 4.3 shows that there is a limitation to increasing the pressure ratio beyond which the cycle efficiency decreases. This is due to the fact that the turbine performance tends to improve at higher pressure ratios at the expense of lower compressor performance.

Equation 4.3 also shows that decreasing the compressor inlet temperature also has the effect of improving the cycle efficiency. Reducing the compressor inlet temperature is possible through different processes, the main of which are:

- **Evaporative cooling**, widely utilized in hot climates with low humidity; the water is sprayed over blocks of fibrous media, and as the airflow passes, the droplets evaporate thus absorbing energy and lowering the temperature.
- **Refrigerated cooling** by using conventional mechanical or absorption cycles. The benefits of this type of cooling have to be examined carefully in relation to the large power consumed by the cooling system. (Boyce, 2002)

Besides improving the cycle efficiency, reduced inlet temperature has an extra benefit of increasing the inlet air density. As turbomachinary is rated per unit volume of flowing fluid, this results in a higher power output. For example, a General Electric (GE) frame 7FA GT rated 174 MW at ISO conditions (15˚C and 60% relative humidity) would produce a maximum of 194 MW at -27˚C while it produces a minimum of 150 MW at 35˚C. (Nakhamkin et al., 2004)

Finally, equation 4.3 shows that increasing the firing temperature also has the effect of improving the cycle efficiency. The main hindrance facing this alternative is the material breakdown at high temperatures. Considerable research is being done in this area by main GT manufacturers.

3.1.2   The Regenerative Cycle

In most GT applications, the exhaust gas has a considerably higher temperature than the air entering the combustion chamber as shown on the T-s diagram in Figure 3.3. The extra heat in the exhaust gas can be used to raise the temperature of the compressed air, thus resulting in fuel savings as shown in the schematic representation in Figure 3.4.
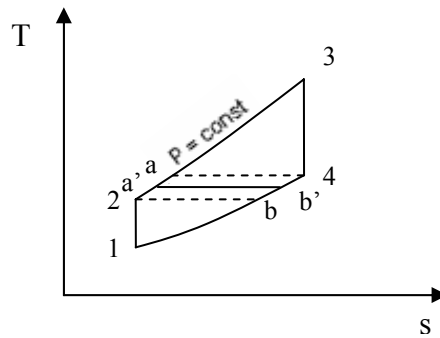
Figure 3.3: T-s Diagram for a regenerative GT cycle.
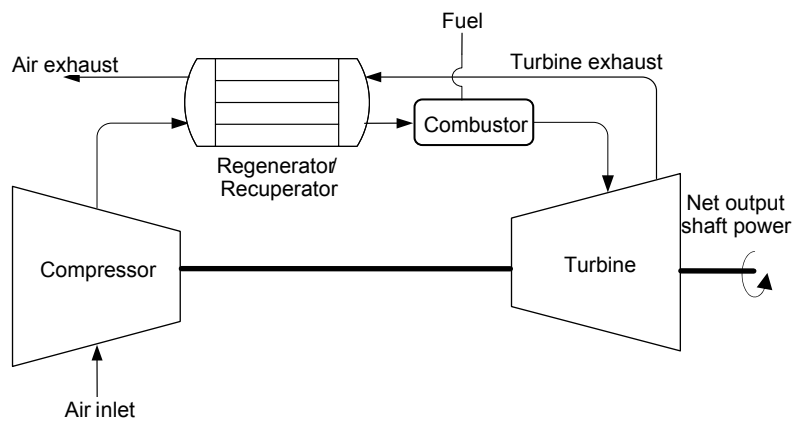
Figure 3.4: Schematic representation of a regenerative GT cycle.

The term "regenerator" refers to a widely used type of heat exchanger where an intermediate medium undergoes cyclic heating and cooling through the alternative passage of hot and cold gas streams. The intermediate media is usually made of a porous material, and it could be either static or dynamic. In the static type, the fluid flow is alternating, whereas the dynamic type includes a rotating drum with continuous fluid flow. A regenerator is usually used where volume compactness is required (Cengel, 1998). The recuperator is another type of heat exchanger widely used in GT applications. In a recuperator, the intermediate medium has a fixed temperature profile, and heat is exchanged through the continuous circulation of the gases in a counter flow arrangement. In this report, the term "regenerator" and "regenerative cycle" are used to describe the process involving the exhaust gas heat recovery system. The exact type of heat exchanger is of little importance for the analysis performed in this report.

Ideally, the cold stream attains the temperature of the inlet hot stream, denoted by (a) and (b) in Figure 3.3, where $T_a = T_4$ and $T_b = T_2$. In reality however, only a limited amount of the available heat is transferred, and the final temperatures reach points (a') and (b'). The regenerator effectiveness is a measure of how much heat was transferred as compared to the maximum possible amount of heat transfer. In a rough estimate, the effectiveness can be expressed as:

$$\eta_{reg} = \frac{T_{a'} - T_2}{T_4 - T_2} \quad \dots\dots\dots\dots\dots\dots\dots\dots\dots\dots\dots \quad 3.4$$

Heat exchange is more effective when the temperature difference between the media is large. Increasing the exchange contact area can improve the heat transfer at the expense of higher exchanger costs. Regenerators require proper maintenance as dirt build up in the flow passages can reduce the exchanger's effectiveness dramatically.

3.1.3 The Intercool / Reheat Cycles

An important factor in the gas turbine design is the compressor power rating compared to that of the turbine. The **work ratio** is used to define the ratio available as shaft work compared to the total power output of the turbine:

$$Work\ Ratio = \frac{Net\ work\ output}{Gross\ work\ output} = \frac{W_{turbine} - W_{compressor}}{W_{turbine}} \quad \dots\dots\dots\dots\dots\dots \quad 3.5$$

There are several ways of increasing the work ratio, the two main ones being **compressor intercooling** and **turbine reheating**, schematically shown in Figure 3.5.
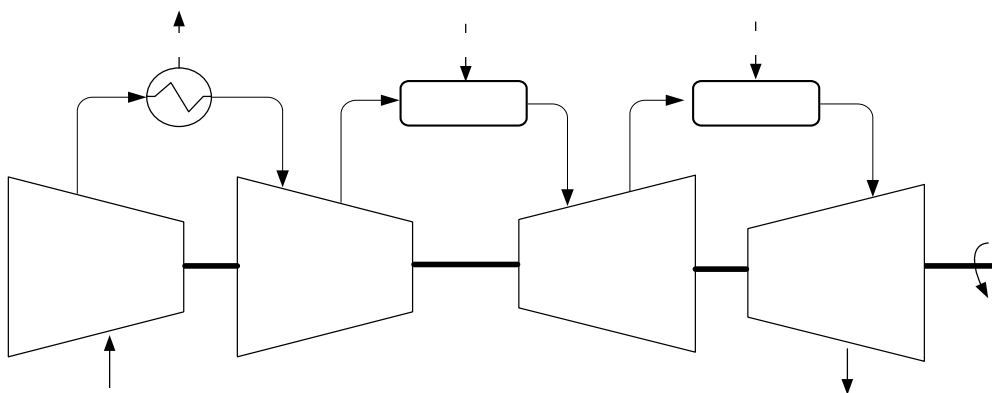
Figure 3.5: *Schematic representation of the GT intercool/reheat cycle. Comp. stand for compressor, comb. for combustor, and HPT and LPT for high pressure and low pressure turbine.*

A good way to explain both processes is to use a T-s diagram (Figure 3.6). The distance between the constant pressure lines are constructed to preserve the isentropic relation for an ideal gas with constant specific heat:

$$\left(\frac{T_1}{T_2}\right) = \left(\frac{P_1}{P_2}\right)^{const} \quad \dots\dots\dots\dots\dots\dots\dots\dots\dots\dots\dots\dots\dots\dots\dots \quad 3.6$$

First the gas is compressed (1-2'), then cooled again to the same temperature as T_1. The second compression stage results in the same pressure increase based on the equation 3.6. With no intercooling, the process would have followed the path 2'-2 in the second stage. Since the distance 2'-2 is larger that 1'-2", the work input required in this compression stage is less using intercooling.
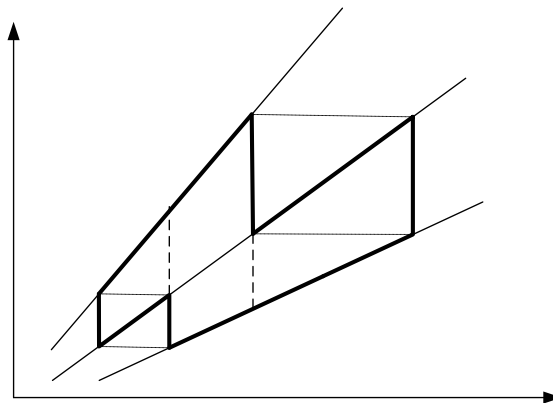
Figure 3.6: T-s diagram for an intercool/reheat cycle. The diagonal lines are constant pressure lines.

A similar argument can be used regarding the expansion process where reheat results in the path 3'-4" being followed instead of 4'-4. Since 3'-4" is larger than 4'-4, the work output from the turbine is higher.

Using both above strategies or one of them would results in increasing the work ratio. However this does not always reflect an increase in efficiency. In fact the above procedures result in an efficiency decrease for a simple cycle without regeneration. This can be also explained on the T-s diagram of Figure 3.6. For the two stage compression process, the gas exits at a lower temperature than the single stage compression. Therefore, fuel has to be used to heat the gas from state 2" to state 2. In the expansion phase, the reheating results in more power output but at the expense of higher exhaust gas temperature which is wasted heat in a simple cycle. With the use of a regenerator or a com-

bined cycle, the intercooling and reheating results in both increased work ratio and efficiency since the exhaust energy is re-used. (Boyce, 2002)

Based on the reheat concept, turbines are usually labeled as high pressure and low pressure turbines (H.P.T. and L.P.T). These turbines can be either mounted on the same shaft or on separate shafts in a so called *split shaft* system where the HPT shaft drives the compressor and the LPT shaft drives the generator.

3.1.4   Other Cycles

There are numerous suggestions on how to improve GT cycle efficiencies and work output ratio. Many of these suggestions however have not become widespread due to economic reasons related to high investment cost. One example of such a cycle is the injection of humidified pre-compressed at the compressor exit and before the combustor (Nakhamkin et al., 2003). This and other modifications are not discussed here and are only mentioned to keep in mind that technological developments other than the ones used in the technology scenarios are also possible.

3.2   CAES Technology

As mentioned in the introduction to this chapter, CAES technology can be considered as a diversion of the GT technology, the main difference being the storage of the compressed air before being expanded in the turbine. This intermediate storage however does have a significant effect on the cycle operation and characteristics. This section starts by giving an overview of the storage caverns before moving to the resulting cycle effects.

3.2.1   Cavern storage

Several options exist for storing the compressed air both above and underground. The range of capacities considered in this analysis however makes underground storage the only feasible and practical solution. The nature of underground storage depends on the geological formation of the area considered. Since the early 1970s, numerous studies have been made on possible underground formations: salt mined caverns, decommissioned oil wells, naturally occurring water aquifers, and even formations induced by

underground nuclear explosions to mention but a few. Two possible operational modes were suggested as well, depending on the type of the formation:

- Constant volume/variable pressure such as in the case of salt caverns.
- Constant pressure/variable volume using a compensating water leg, such as in the case of aquifers.

Out of all the suggested formations, only mined salt caverns have been implemented in utility scale CAES applications. The geological nature of the ground in Denmark allows for the mining of such salt caverns, and two facilities are already being used for the storage of natural gas at Ll. Torup and Stenlille in Jylland and on Sjælland respectively. Besides the geological nature of Denmark, there are several other reasons why salt mined caverns are preferred:

- Salt caverns have the advantage of being air tight, with no significant leakage losses reported. (Crotogino et al., 2001)
- The exact size of the storage can be mined at the proper depth that matches the desired operational pressure range.
- The total cavern volume can be divided into several compartments. This has proven to be particularly useful in Huntorf for example, especially that the installed compressor capacity is usually not enough to fill a cavern starting at atmospheric pressure after maintenance. Pressure withdrawn from the neighboring compartments can save the need to utilize often costly and time consuming mobile compressors. (Crotogino et al., 2001)

A salt cavern is usually constructed by injecting water underground and retrieving the resulting brine out. The depth of the cavern is chosen to ensure stability at both atmospheric pressure as well as maximum operational pressure. The cavern size is to be chosen such that it does not exceed safe expansion rates that could affect the cavern walls. In Huntorf for example, the maximum pressure drop rate is limited to 15bars/hour. (Crotogino et al., 2001)

The cavern wells are usually fitted with steel pipes encased by concrete. This limits the maximum air temperature that can be injected to the cavern, as higher temperatures result in pipe expansion and increased stress on the concrete casing. A second reason to

limit the injected air temperature relates to the mechanical properties and the water content of the cavern. For these reasons, it is customary to after-cool the compressed air to acceptable temperatures before being injected to the cavern. (ERDA, 1976)

Inside the storage, heat exchange occurs between the compressed air and the cavern walls as long as there is a temperature difference between the two. Typical cavern wall temperatures have been found to be 35°C in Huntorf. It was also found that only the outer layer of the cavern walls within a 1 meter range is involved in the heat exchange. In this regards, the cavern walls can be regarding as a heat source/sink that has a fixed temperature. The exact heat transfer rate depends on the specific geometry of the cavern and the exposed surface area. As the air in the storage cools down after being compressed, the pressure decreases proportionally at a constant volume. This adds another reasons for cooling the air before injecting it, namely to increase the available storage capacity during injection. (Crotogino et al., 2001)

The air or gas coming out of the cavern usually has high impurity and water contents. This can be corrosive for the well piping and the turbine blades. In the Ll Torup natural gas storage for example, the gas is purified after being expanded from the storage and before being dispatched in the natural gas network. Uncoated steel pipes initially used had to be replaced in the Huntorf plant months after operation started and fiber glass reinforced plastic (FRP) were used instead. No significant corrosion due to air impurities has been reported in the turbine though. (Crotogino et al., 2001)

3.2.2   The CAES Cycle

From a thermodynamic perspective, the main difference between a standard GT cycle and a CAES cycle is the cooling of the air prior to its injection in the cavern. Besides, as the air expands at a constant volume, its temperature drops further. These factors make the CAES cycle less efficient in terms of fuel consumption as an increased amount of heat is needed to raise the air temperature to the turbine inlet temperature.

The higher the compression ratio, the more heat is lost. Therefore, a tradeoff exists between increasing the pressure ration to improve turbine performance and minimizing compression heat losses. This results in optimal pressure ratios that are lower for CAES

than for GT cycles. Figure 3.7 shows the efficiency variation with the pressure in the cavern. At low pressures, the turbine's efficiency is quite low, whereas under high pressures, the compression heat losses are quit high.
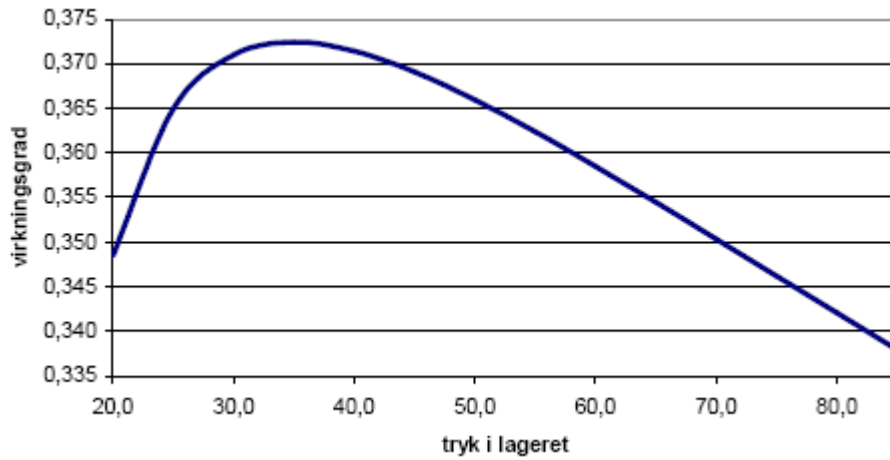
Figure 3.7: *The GT efficiency of a CAES plant under varying storage pressures (X-axis) found by statistical simulation. (Brix and Szameitat, 2003)*

The term efficiency described above is described in a similar manner to the GT heat engine efficiency as described in equation 3.1. For a CAES plant, the net work output would be the difference between the electricity produced and the electricity consumed:

$$\eta_{GT,CAES} = \frac{El.Out - El.In}{Fuel\ Heat} \ \dots\dots\dots\dots\dots\dots\dots\dots\dots\dots\dots\dots\dots \ 3.7$$

The above expression however does not take into account the fact that the compression and expansion are occurring at varying time. In such a case, the source of the Electricity input is important to consider in defining the overall system efficiency. Whether the electricity comes from thermal power plants or from otherwise wasted wind energy can change the way the GT CAES efficiency is perceived, and therefore the above value should not be used as the only criteria to judge CAES performance.

The definition of the storage efficiency can be a demanding task thermodynamically especially that the potential energy contained in the air (exergy) depends on the process used during the expansion. For this reason, the following energy ratios are used to describe the system:

$$El.Ratio = \frac{El.\,Input}{Unit\,El.\,Output} \quad \dots\dots\dots\dots\dots\dots\dots\dots\dots\dots\dots 3.8$$

$$Fuel.Ratio = \frac{Fuel\,Thermal.\,Input}{Unit\,El.\,Output} \quad \dots\dots\dots\dots\dots\dots\dots\dots\dots 3.9$$

$$Heat\,Ratio = \frac{Waste\,heat.}{Unit\,El.\,Output} \quad \dots\dots\dots\dots\dots\dots\dots\dots\dots 3.10$$

Note that the waste heat includes the heat from compression and the exhaust heat from the turbine with temperatures above ambient temperature. In this report, the above values are always reported after running a cycle starting with an empty storage, total fill up, wait until the air temperature attains the cavern wall temperatures, and then expand back to empty storage.

3.3   Existing CAES plants

The concept of storing compressed air on a small scale in rock caverns has been long used by the mining industry to operate pneumatic equipment. The first patents to suggest the use of compressed air storage for electricity power generation were attributed to Gay in the United States (1948), Stal Laval in Sweden and The U.K. (1952), and Djordjevic in Yogoslavia (1950). Since that time, numerous studies have been made in several countries for assessing the feasibility of potential CAES projects. For example, plans were announced in 1972 to build the "world's first pumped air storage plant" by Sydsvenska Kraft A.B. near Växjo, Sweden. Similar plans were further elaborated when the Swedish State Power Board announced successful test borings north of Norrköping. Yet both plants never materialized for various economic reasons. (ERDA, 1976).

Today, two CAES plants exist in the world, and this section would be confined to the description of these two plants. It is noted however that several plans for constructing new CAES plants are still actively pursued, most notably of which is a project Norton, Ohio, USA, with a turbine capacity of 2700 MW[2]. The two existing CAES plants are:

[2] Further description of this CAES project is found on the website of the CAES development company L.L.C. on www.caes.net

      1 – A 280 MW plant in **Huntorf**, Germany

      2 – A 110 MW plant in McIntosh, **Alabama**, United States.

3.3.1   The Huntorf Plant

All data and figures in this section are based on Crotogino et al., 2001. Figure 3.8 shows a schematic representation of the Huntorf plant. The pant was commissioned in 1978 and has completed more than 25 years of successful operation. The plant is mainly de-signed to store daily off-peak power and produce during peak hours in a system domi-nated by thermal power plants. The compressor is rated at 60 MW and consists of two stage compression with inter and after-cooling. The turbine is rated at 290 MW and consists of a HPT and a LPT. Both the turbine and the compressor are connected to the same motor/generator unit.
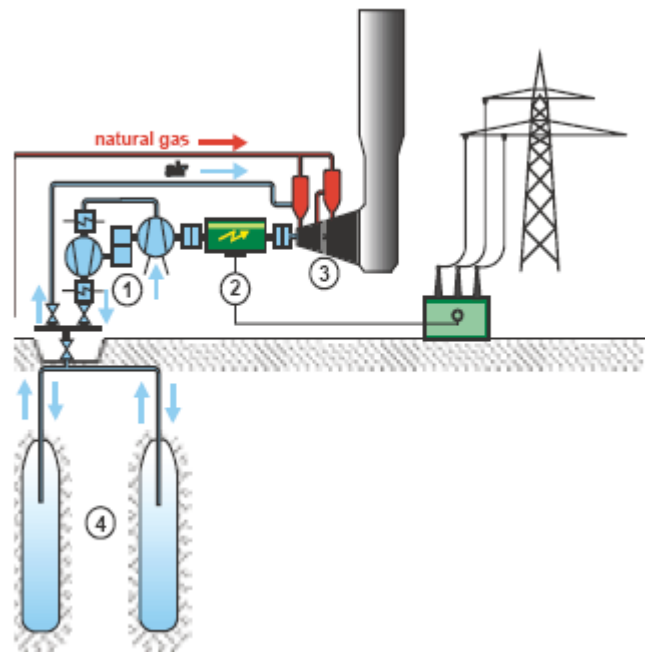
Figure 3.8: *Schematic representation of the Huntorf CAES plant. Note the 2 stage compression and the single generator/motor unit.*

The storage consists of two compartments with a total size of 310,000 m^3. The com-pression time goes up to 12 hours, and the expansion time up to 3 hours. Initially, the plant had around 200 starts per year for both compression and expansion. In 1985 how-ever, the electricity system was connected to a larger network area that included

pumped hydro storage, and the number of starts dropped to around 90 per year in 2002 (Crotogino, 2001).

Experience from Huntorf has shown that salt caverns constitute a very good medium for CAES applications. Surveys of the cavern walls after 20 years of operation has shown practically no deviation compared to the original conditions. Table 3.1 summarizes the main characteristics of the CAES plant at Huntorf.

Compression	Capacity	60	MW
	Mass flow rate	108	Kg/s
	Expected time	12	hours
Expansion	Capacity	290	MW
	Mass flow rate	417	Kg/s
	Expected time	3	hours
Storage	Depth – top	650	m
	Depth – Bottom	800	m
	Volume	310,000	m^3
	Minmum Pressure	43	bar
	Maximum Pressure	70	bar
	Maximum Pressure reduction rate	15	bar/hour

Table 3.1: *Summary of main Technical Characteristics of the Huntorf CAES plant.*

3.3.2   The Alabama Plant

The Alabama CAES plant was commissioned in 1991. The plant has a compressor capacity around 50 MW and a turbine capacity of 110 MW. The plant is constructed in connection with a 100 MW coal plant and acts as a regulating capacity to between the coal plant's capacity and the electricity demand. The Alabama plant has a better performance than the Huntorf for several reasons:

1. Compression is performed on 4 stages rather than 2 stages.
2. A regenerator is used to utilize the turbine exhaust heat for preheating the expanding air from the cavern. This results in major fuel savings.
3. The storage size at Alabama is 504,000m^3 with a turbine extraction rate of around 154m^3. This result in lower pressure drop rates in the cavern compared to Huntorf, which leads to more moderate temperature drops during expansion.

For these reasons, the Alabama plant is considered is treated as the base technology scenario in this report. Figure 3.9 is a schematic representation of the plant along with approximate thermodynamic properties at the various notes. These values are used as a main reference in the modeling stage and the figure would be referred to quite often.
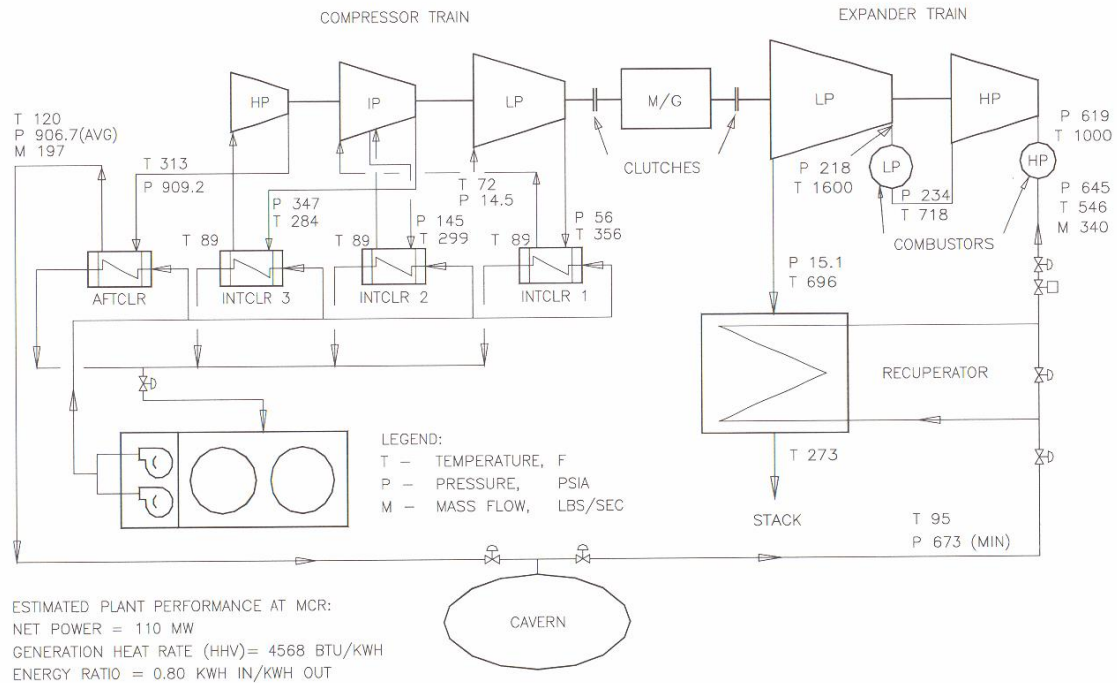
Figure 3.9: The Alabama plant schematic representation with main thermodynamic properties. Figure taken from (Boyce , 2002) where it is adopted from Energy Storage and Power Consultants, Inc. (ESPC) which has experience in "engineering, constructing, testing, and operating" the Alabama CAES plant.(www.espcinc.com)

4. Model Description

For performing the analysis, a thermodynamic model of a CAES plant was developed. The model can be divided into two sub-categories: Thermodynamic model, and operational model. The thermodynamic part deals with the technological behavior of the individual components and their interaction with each other in the overall system. The operational part deals with the strategy under which a plant operates to maximize profit. The model was implemented in matlab due to its ability to handle matrices easily.

This chapter describes the main assumptions and procedures used the CAES plant modeling. Section 4.1 describes the main plant configuration and the individual components description as implemented in the model. Section 4.2 then shows some sample technical results from the built model in particular in relation to literature available about the Alabama CAES plant. Finally, section 4.3 describes the main operational strategy employed to simulate the plant's operation on the market.

4.1 Technical Model

Figure 4.1 shows the overall CAES plant configuration constructed based on the Alabama plant. The plant consists of a 4 stage compressor with intern and after cooling. The gas turbine is divided into 2 stages, a high pressure and low pressure turbine (HPT and LPT). A regenerator is used to preheat the air leaving the cavern and save fuel demand. Both compressor and turbine are connected to the same motor/generator set. In order to describe the overall behavior of the CAES plant at various capacities and specifications, a modular approach in constructing the technical model. Each component is modeled separately, and the components are later assembled by using the exit state of one component as the inlet state to the other. The plant operation is based on a user specified time step. The smaller the time step, the more detailed the results are on the expense of longer simulation time. For efficiency simulations, a time step around 60 seconds can be used, whereas for annual simulations a larger time step can be used.
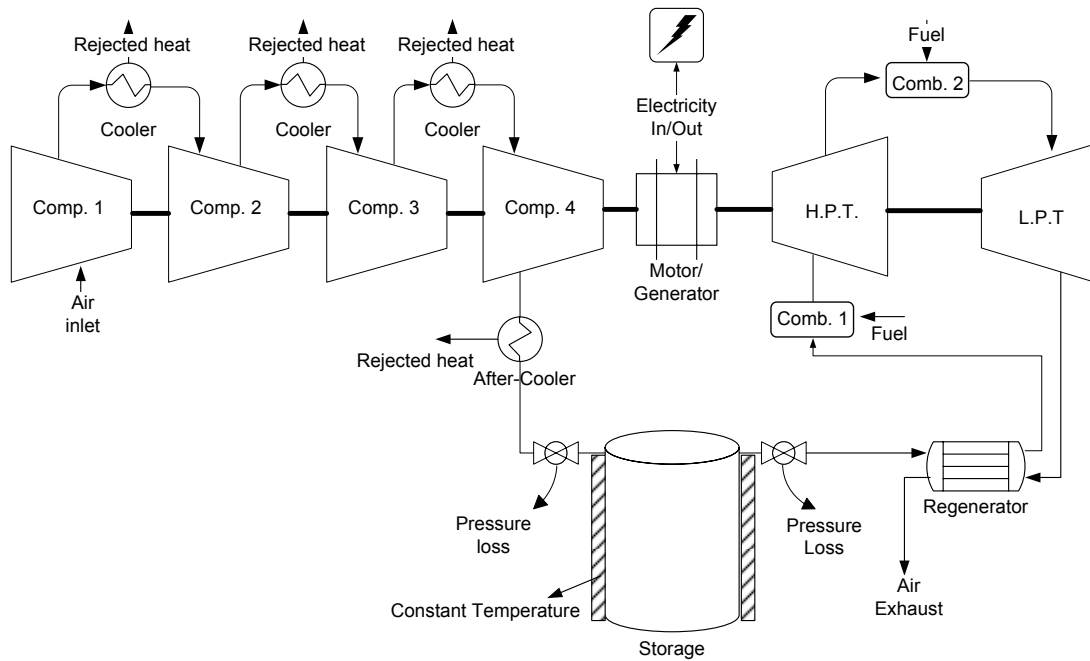
Figure 4.1: *The schematic diagram of the main CAES plant configuration modeled.*

It should be noted here that the compressor and turbine are assumed to operate against varying pressure without changes in their performance. Throttling valves can be used to keep the pressure operation range constant, however this is not implemented at this stage. The throttling valves shown in Figure 4.1 are used only to model pressure drop in the piping system. The exact variation of the compressor and turbine behavior operating at various pressures is an area that requires further investigation. The effect is not expected to be very large though. (Cohen, 1987) suggests that the main compressor properties remain essentially that same as long as the mass flow rate and exit pressure vary within a certain range from the design point.

What follows is a description of the following main components used in the overall plant build-up:

- Working fluid
- Compressor
- Inter-Cooler
- Storage
- Combustor
- Turbine
- Regenerator

4.1.1 Working fluid

The assumptions regarding the working fluid – air in this case – are crucial for the modeling of the rest of the components. Two main simplifying assumptions are made regarding air properties:

1. Ideal gas behavior.
2. Constant specific heat for the calculation of internal energy and enthalpy.

Ideal Gas Behavior

Ideal gases are assumed to follow the ideal gas *equation of state*:

$$Pv = RT \ \dots\dots\dots\dots\dots\dots\dots\dots\dots\dots\dots\dots\dots\dots\dots 4.1$$

Where:

- P is the pressure [KPa]
- v is the specific volume [m^3/Kg]
- R is the gas constant [KJ/Kg-K]
- T is the absolute temperature [K]

Real gases diverge from the ideal gas assumption by a compressibility factor Z, expressed as:

$$\frac{Pv}{RT} = Z \ \dots\dots\dots\dots\dots\dots\dots\dots\dots\dots\dots\dots\dots 4.2$$

Charts giving the value of Z are available based on the reduced temperature and pressure (the ratio between the temperature/pressure and the corresponding value at the critical state). Checking such a chart for the temperatures and pressures ranges involved in CAES (up to 80 bar and 1200 K) shows that Z indeed remains relatively close to 1, thus justifying the ideal gas assumption[3].

Constant Specific Heat, Internal Energy and Enthalpy

Specific heat is defined as the amount of energy needed to raise the temperature of a gas by one degree Celsius (in SI units). Since gases expand with temperature increase if the container allows them to, two specific heat values are defined for gases: constant volume (C_v) and constant pressure (C_p). The constant volume C_v is lower than C_p since at

---

[3] A Compressibility chart is available on page 123 in (Gresh, 2001), and the critical values of temperature and pressure for air are tabulated on page 122 of the same reference.

constant pressure extra energy is needed to support the gas expansion and the temperature increase.

For a real gas, the internal energy and enthalpy are a function of temperature, pressure, and specific volume:

$$u = u(T,v) \dots\dots\dots\dots\dots\dots\dots\dots\dots\dots\dots\dots\dots 4.3$$

$$h = h(T,P) \dots\dots\dots\dots\dots\dots\dots\dots\dots\dots\dots\dots\dots 4.4$$

For an ideal gas however, *u* and *h* can be reduced to a function of temperature only, and the exact expression for internal energy and enthalpy change is expressed as:

$$u(T) - u_{ref} = \int_{Tref}^{T} C_v dT \dots\dots\dots\dots\dots\dots\dots\dots\dots\dots 4.5$$

$$h(T) - h_{ref} = \int_{Tref}^{T} C_p dT \dots\dots\dots\dots\dots\dots\dots\dots\dots 4.6$$

In order to integrate equations 4.5 and 4.6, and equations expressing C_v and C_p in terms of temperature are needed. Approximate relations from empirically generated data are constructed using curve fitting methods to describe the dependency of C_v and C_p on temperature. For air, a third order expression valid between 300 K and 1200 K is available from (Sonntag et al., 2004; page 659):

$$C_p = C_o + C_1\theta + C_2\theta^2 + C_3\theta^3 \dots\dots\dots\dots\dots\dots\dots\dots 4.7$$

Where

- $\theta = \dfrac{T[K]}{1000}$

- C_o, C_1, C_2, C_3 = 1.05, -0.365, 0.85, and -0.39 respectively

This expression can be readily substituted in equation 4.5 and integrated. However, another approach that gives almost similar accuracy is to assume a constant specific heat value calculated from expression 4.7 at the average temperature:

$$T_{av} = \frac{T_{ref} + T}{2} \dots\dots\dots\dots\dots\dots\dots\dots\dots\dots\dots\dots 4.8$$

The later approach is used in the model for calculating C_p. C_v is deduced from C_p using the ideal gas relation:

$$C_v = C_p - R \dots\dots\dots\dots\dots\dots\dots\dots\dots\dots\dots\dots\dots\dots\dots 4.9$$

Where R is the gas constant; R = 0.287 KJ/Kg-K.

The specific heat ratio is then found as the ratio:

$$k = \frac{C_p}{C_v} \dots\dots\dots\dots\dots\dots\dots\dots\dots\dots\dots\dots\dots\dots 4.10$$

Using the calculated specific heat values, and given the reference internal energy and enthalpy values (u and h), it is possible to calculate the corresponding u and h at any other temperature. For example, defining the reference state at $T_{ref} = 298.15$ and using the above relations, the resulting enthalpies and errors compared to thermodynamic tables are shown in Table 4.1, and the relative error is shown to be below 0.01% even for very large temperature differences.

T	h (tables)	h (model)	Relative Error
[K]	[KJ/Kg-K]	[KJ/Kg-K]	%
280	280.39	280.39	
600	607.32	607.026	-0.048%
1000	1046.22	1045.3	-0.088%

Table 4.1: *Enthalpy values calculated based n constant specific heat assumptions compared to thermodynamic tables.*

4.1.2 Compressor

Isentropic compression (internally reversible and adiabatic) can be considered as the ideal compression process. On a T-s diagram, this process is represented by a vertical straight line. The efficiency of a compressor can thus be taken as the ratio depicting how well a compressor follows the ideal isentropic process.

Applying the first law of thermodynamics for a control volume around the compressor, and assuming an adiabatic process, the energy gained by the air, also known as the head, can be shown to equal the difference in the air enthalpy:

$$H = h_{exit} - h_{inlet} = C_p (T_{exit} - T_{inlet}) \dots\dots\dots\dots\dots\dots\dots 4.11$$

The isentropic efficiency is consequently the ratio of the isentropic head to the actual head needed to compress the air:

$$\eta_{comp,is} = \frac{H_{is}}{H_{actual}} = \frac{C_{p,is}(T_{exit,is} - T_{inlet})}{C_{p,actual}(T_{exit,actual} - T_{inlet})} \quad \dots\dots\dots\dots\dots\dots\dots 4.12$$

For an ideal gas with constant specific heats undergoing an isentropic process, the following relation holds:

$$\frac{T_2}{T_1} = \left(\frac{v_2}{v_1}\right)^{k-1} = \left(\frac{P_2}{P_1}\right)^{(k-1)/k} \quad \dots\dots\dots\dots\dots\dots\dots\dots\dots\dots\dots 4.13$$

k being the specific heat ratio assumed to be constant at the average temperature.

The compressor matlab function implements the above relations, and given the isentropic efficiency, pressure ratio, and inlet air state, the exit state is returned.

The isentropic efficiency does not account for mechanical losses in the driving motor and shaft. To include these, the actual head requirement is divided by a user defined mechanical efficiency η_{mech}.

It is possible to assume a polytropic compression as the ideal process instead of an isentropic compression. A polytropic process is an internally reversible process that includes heat transfer. Due to the cooling effect, compressor polytropic efficiency is usually higher than the isentropic efficiency. For a polytropic process, a polytropic exponent *n* is used in equation 4.13 instead of the specific heat ratio. Although not used in the model, the compressor function can return the exit state if the polytropic exponent and efficiency are used as an input instead of the isentropic values. It is however an industry practice to use isentropic values for single stage and air compressors and to use polytropic values for all other applications. (Gresh, 2001)

In order to minimize power consumption, it is customary to perform multi-stage compression with intercooling as discussed in section 3.1.3. It is important to note here that the overall compressor train efficiency is not the product of the individual efficiencies.

An overall isentropic efficiency can be defined if the actual total head input is compared to the corresponding isentropic head for a single stage compression, but that value is very sensitive to the cooling procedure and is application specific rather than manufacturer specified. Thus the only value used in this report is the individual compressor isentropic efficiency.

4.1.3 Turbine

The turbine component is described in a very similar way to the compressor. The turbine isentropic efficiency is defined as:

$$\eta_{is} = \frac{Actual\ air\ head}{Isentropic\ air\ head\ loss} = \frac{h_{inlet} - h_{exit}}{h_{inlet} - h_{exit,is}} \quad \dots\dots\dots\dots\dots\dots\text{4.14}$$

Which can be reduced to:

$$\eta_{is} = \frac{C_{p,actual}(T_{inlet} - T_{exit,actual})}{C_{p,is}(T_{inlet} - T_{exit,is})} \quad \dots\dots\dots\dots\dots\dots\dots\dots\dots\text{4.15}$$

Using the isentropic process relations in equation 4.13, and given the pressure drop ratio and inlet condition, the turbine exit condition is defined. The actual head output is multiplied by a user defined mechanical efficiency η_{mech} to account for the generator and shaft mechanical losses.

4.1.4 Cooler

The compressor inter and after coolers are modeled as a heat exchanger. The air is assumed to exchange heat with a cooling fluid (water in this case) whose inlet and exit temperatures are user specified. Water is assumed to enter at ambient temperature, and its mass flow rate is changed to keep its exit temperature below boiling point. The air inlet temperature and flow rate are assumed to be known. Using the following relations, the required cooling fluid flow rate and the resulting air exit temperature are calculated:

$$\varepsilon = \frac{Actual\ heat\ transfer}{Maximum\ possible\ heat\ transfer} = \frac{\dot{Q}}{\dot{Q}_{max}} \quad \text{...............} \quad 4.16$$

The maximum possible heat transfer depends on the limiting minimum heat capacity of either fluids, expressed as:

$$\dot{Q}_{max} = C_{min}(T_{hot,in} - T_{cold,in}) \quad \text{..................................} 4.17$$

Where C_{min} is the minimum heat capacity between the two fluids. $C = \dot{m}\,C_p$, $\dot{m}$ being the mass flow rate and C_p the specific heat.

4.1.5 Combustor

The combustor function returns the heat input amount given the required temperature increase by finding the enthalpy difference. The returned value is in MJ, and dividing by the fuel's heating value allows finding the amount of fuel used. Data from the Alabama CAES plant in Figure 3.9 shows a certain pressure loss across the combustor, and this is modeled as a user specified pressure ratio.

4.1.6 Regenerator

The regenerator is treated as a heat exchanger using the same relations applied in the cooler. The only difference in the case of a regenerator is that the mass flow rate of both fluids is usually known (in this case being equal), while the exit temperature of both fluids is unknown. Besides, data from Figure3.9 suggest a pressure loss across the regenerator for the high pressure stream (coming from the storage), and this is modeled as a user specified pressure ratio.

The regenerator matlab function returns the exit state of both fluids and the amount of energy saved in MJ. As in the case of the combustor, dividing the saved energy by the fuel heat value gives the amount of saved fuel.

4.1.7   Storage

The storage is modeled as a constant volume container whose walls remain at a constant temperature thus acting as a heat source/sink. The required input variables are the inlet/exit mass flow rate and fluid characteristics, and the storage wall temperature and the heat exchange rate between the air and the walls. The resulting output is the air state (temperature and pressure) in the storage at each point in time

As mentioned in 3.3.1, the air leakage from the storage is too small and can be neglected. The continuity equation for the storage can be then expressed as:

$$\frac{dM_{st}}{dt} = \overset{\bullet}{m}_i - \overset{\bullet}{m}_e \ \dots\dots\dots\dots\dots\dots\dots\dots\dots\dots\dots\dots\dots \ 4.18$$

The first law of thermodynamics for the storage control volume results in the second equation:

$$\frac{dU}{dt} = \overset{\bullet}{Q}_{walls} + \overset{\bullet}{m}_i \, h_i - \overset{\bullet}{m}_e \, h_e \dots\dots\dots\dots\dots\dots\dots\dots\dots\dots.4.19$$

$$\overset{\bullet}{Q}_{walls} = K_{heat} \cdot M_{air} \left(T_{air} - T_{walls} \right) \dots\dots\dots\dots\dots\dots\dots\dots\dots \ 4.20$$

With the temperature profile calculated using 4.19, the pressure profile can be deduced using the ideal gas equation of state (equation 4.1).

4.2   Technical Model Performance

The current day technology (CDT) is based on the information available about the Alabama plant from figure 3.9 and data used in (Brix and Szameitat, 2003). The model is calibrated to match both sets of data as close as possible. For calculating the efficiency and performance indicators, the model is run with a time resolution of 1 minute starting with storage at 50 bars. After reaching 75 bars, a certain time is elapsed so that the compressed air reaches the temperature of the cavern walls. Finally, the air is expanded again to 50 bars.

The main model inputs and the resulting performance values are summarized in Table 4.2 in comparison to literature values. The heat ratio is calculated with 35°C as a reference temperature. The inlet ambient temperatures are the same as Figure 3.9. The result-

ing electricity and fuel ratios are quit close to the literature values. The minor difference is acceptable especially that the plant performance is variable and even some input values are reported with slight difference in the two main references.

		Literature	Reference	CD Tech	Units
Compressor	nmech			95%	
	nis	82%	[1]	82%	
	mrate	96	[2]	96	[Kg/s]
Cooler	effectiveness	-		90%	
	Ti	32	[1]	32	[C]
HPT	nmech			95%	
	nis	86%	[1]	86%	
	mrate	154	[1]	148	[Kg/s]
	Ti	538	[1]	538	[C]
	Pratio	0.378	[1]	0.378	
LPT	nis	90%	[1]	90%	
	Ti	871	[1]	871	[C]
Combustor	Pratio	0.96	[1]	0.96	
Regenerator	effectiveness	0.7		0.7	
	Pratio	0.96	[1]	0.96	
	Volume	504,000	[2]	504,000	m3
Cavern	Pmax	78	[2]	75	Bar
	Pmin	50	[2]	50	bar
Results	El Ratio	0.8	[1]	0.7401	
	Fuel Ratio	1.339	[1]	1.2898	
	Heat Ratio			0.8352	
	GT Efficiency			20.15	
	Comp Time	42	[2]	40.95	hours
	Exp Time	26	[2]	25.633	hours
	Com capacity	50	[2]	48.713	MW
	Turb Capacity	110	[2]	109.73	MW

Table 4.2: *Current Day Technology base model input values and resulting performance [1] refers to Figure 3.9 and [2] refers to (Brix and Szameitat, 2003).*

Figure 4.2 shows the variation of the cavern pressure and temperature during the compression/expansion cycle. Note that as the pressure increases, the temperature increase slows down and in fact starts decreasing gradually. Similarly, the temperature drops faster during the initial expansion phase. This is a direct consequence of the heat exchange factor chosen in the cavern. This behavior is confirmed with simulation results found in (Brix and Szameitat, 2003).
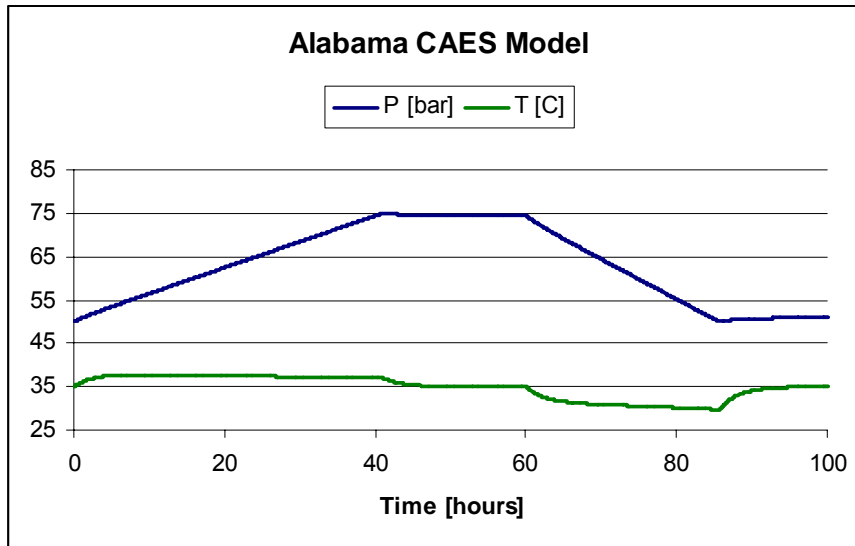
Figure 4.2: *Model results for the variation of the storage temperature and pressure over an operational cycle.*

Figure 4.3 shows the variation of the electricity ration, fuel ratio, and GT efficiency for various turbine mass flow rates. It can be seen that the system performance drops at higher turbine flow rates, one of the main reasons for that being the lower temperature drop leading to a higher fuel ratio.
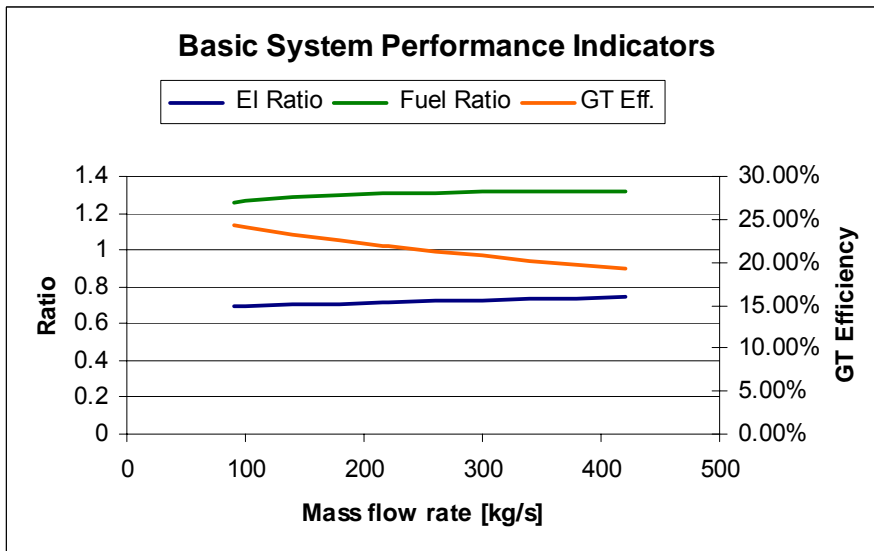
Figure 4.3: Basic system performance indicators for the CDT model at various turbine capacities, the main other capacities being the same as the Alabama plant.

4.3　CAES Operational Strategy

The technical model described in sections 4.1 and 4.2 is used within an operational model that attempts to find the potential business opportunities for a CAES plant on the electricity market. The model uses a deterministic electricity price time series as the basis of calculation with a time step of 1 hour

For a standard electricity power plant, profitable operation requires that the price per unit electricity sold exceeds the marginal cost of production (M.C.) of that unit. Four main operational costs are identified in the model:

1. **Fuel Cost:** The fuel cost refers to the natural gas used during operation. The cost is represented by a fixed average annual value.

2. **Electricity Cost:** This represents the cost of the electricity bought for the compressor, and is calculated based on the electricity price time series.

3. **Startup Cost:** A startup cost is associated with both compressor and turbine, and it is meant to include startup fuel consumption and machine wear. The startup fuel consumption is given the same cost as the fuel costs specified earlier, while the machine wear is given a fixed average value. In order to determine whether the unit has started up or not at an hour *(i)* the following binary expression is used:

$$CompStartupCheck = (1 - CompStatus(i-1)) \cdot (CompStatus(i)) \ldots\ldots..4.21$$

$$TurbStartupCheck = (1 - TurbStatus(i-1)) \cdot (TurbStatus(i)) \ldots\ldots.4.22$$

   Where *CompStatus* and *TurbStatus* are two time series determining the operational status of the compressor and the turbine, (1 = on; 0 = off).

4. **Other Operational Costs:** The other operational costs are given a fixed average value that can include power consumption from auxiliary units (pumps, fans) and machine wear costs.

The variable annual operational income (VAOI) is then defined as the difference between the income from electricity sale on one hand and the operational costs on the other. A positive VAOI reflects a profitable operation.

The factors included in the marginal cost calculation make it time dependant with the price of the purchased electricity playing a major role. In other words, for every electricity purchase price, there exists a corresponding electricity bidding price. This creates a difficulty in the optimization strategy especially that compression occurs over a number of hours with a range of electricity prices. For finding the optimum bidding strategy and the resulting VAOI, the following simulation strategy is implemented:

1. The plant operator specifies a **maximum buying price**, and a certain **minimum bidding price**.
   The simulation is performed over the specified period, and the resulting VAOI is recorded.

2. Step 1 is repeated with new values for buying and bidding prices until the optimum buying and bidding prices leading to maximum *Period Profit* are determined, which is considered the solution for the corresponding period.

3. The storage content at the end of the simulation period is used as the income to a second iteration which ensures that the storage content is the same at the beginning and the end of the period.

The price time series is usually seasonal in nature, and the optimal bidding strategy can vary from one season to the other. In the Nordic system, prices in the winter for example tend to be higher than prices in the summer due to electricity used for heating, and if the same buying and bidding prices used for winter are applied in the summer, the plant could end up only compressing with no subsequent expansion, and hence no operation. The opposite is also true in the case of using the summer's buying/bidding prices for the winter, where the turbine would operate until the storage is empty with no chance of refilling again. For this reason, the optimum strategy is calculated on a seasonal basis first before finding the overall VAOI.

During operation, it is expected that the electricity system prices would react to the extra demand/supply induced by the CAES plant. This is modeled by including a price dependency factor for both supply and demand. The price is altered based on the following relation:

$$\Pr ice(i) = \Pr ice(i) - SupplyDepFactor \times TurbCapacity \;\ldots\ldots\ldots\ldots\text{4.23}$$

$$\Pr ice(i) = \Pr ice(i) + DemandDepFactor \times CompCapacity \;\ldots\ldots\ldots\text{4.24}$$

Where SupplyDepFactor and DemandDepFactor represent the price sensitivity in DKK/MWh extra supply or demand. Both f*actors* can be approximated from historical data using statistical methods.

The simulation assumes that the plant operates at full capacity only. No part-load operation is allowed at this stage. In practical cases however the plant can be constructed in a modular manner with separate operating units. This can be simulated by running the smallest operating unit first. The resulting price time series can then be used to judge the operation of the later units in a consequent manner until the full capacity is reached.

Besides the spot market, the plant operator has the option of bidding on regulating power market. This is particularly true for a CAES plant that has relatively fast regulating power ability where the compressor starts up within 20 seconds and the turbine within around 8 minutes (Girsh, 2001). Since the system price series are assumed to be deterministic, it is up to the user to assume the prices that could match the desired power market. For example, it is possible to use historic time series of the regulating power market prices instead of Elspot prices.

In real life however, the actual production decision is more complicated, and more thorough simulations and experience are needed to make the proper bidding choice. This could be an interesting topic for a further research study.

5. Analysis

This chapter presents the main analysis assumptions and results from simulations using the model described in Chapter 4. In order to examine potential CAES business opportunities, three main technological scenarios and a future electricity system scenario are used as described in Chapter 2. Sections 5.1 and 5.2 start by further specifying the characteristics of the future technical and electricity system scenarios respectively. Section 5.3 presents the main simulation results while section 5.4 examines the potential CAES feasibility. Finally, section 5.5 discusses the sensitivity of the investment decision to some factors like extreme weather years and various investment costs.

5.1 Technology Scenarios

Section 4.2 presented the technical specifications of the model used to describe the Alabama plant. This model is labeled **Current Day Technology** (CDT) and is used as the basis for the two other technical models. The **State of the Art Technology** (SOAT) is based on the General Electric 109H system gas turbines. This advanced turbine model has a firing temperature that reaches 1430°C and a combined cycle efficiency that exceeds 60%. The firing temperature for both the LPT and the HPT in the SOAT scenario are multiplied by a factor of 1.64 compared to the Alabama CDT scenario. Finally, the **Advanced Technology** (AT) is an attempt to reduce the fuel consumption of the SOAT by having a regenerator with 0.9% effectiveness and having a heat storage where 50% of the heat rejected by the compressor can be re-used to preheat the air during expansion. Table 5.1 summarizes the main changes in technical inputs compared to the CDT base values shown in table 4.2

	CDT	SOAT	AT
HPT Ti	538	882	882
LPT Ti	871	1428	1428
Regenerator Effectiveness	70%	70%	90%
Waste heat utilization	None	None	50%

Table 5.1: *Main changes in the SOAT and AT scenarios compared to the CDT base model.*

With a higher firing temperature, the SOAT and the AT have a higher power output for the same air mass flow. Figure 5.1 depicts the turbine capacity corresponding to the same air mass flow rate for the CD and the SOA technology.
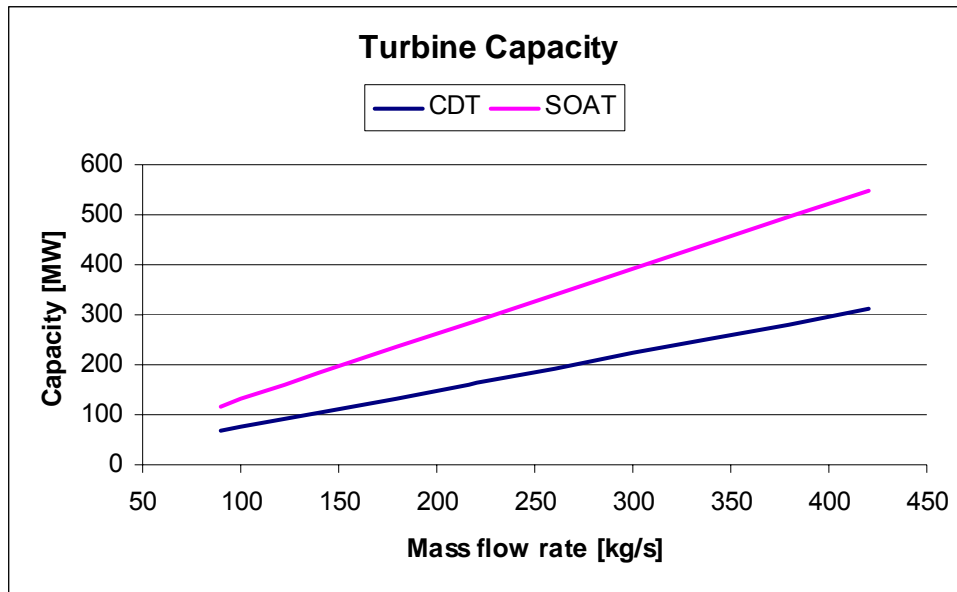
Figure 5.1: For the same air mass flow rate, turbines at higher firing temperature give a higher power output as shown by comparing the CDT and the SOAT results

This higher power output allows for a lower compressed air demand per electricity output unit thus meaning a lower electricity ratio (El_{in}/El_{out}). The higher firing temperature however leads to an increase in the amount of fuel needed giving a higher fuel ratio ($Fuel_{in}/El_{out}$). With the help of the recuperator, majority of the heat is re-utilized, and a improvement in the overall gas turbine efficiency (η_{GT}) is achieved. The heat ratio is further reduced in the AT compared to the SOAT because of the improved regenerator and waste heat utilization. These results are depicted in Figure 5.2.
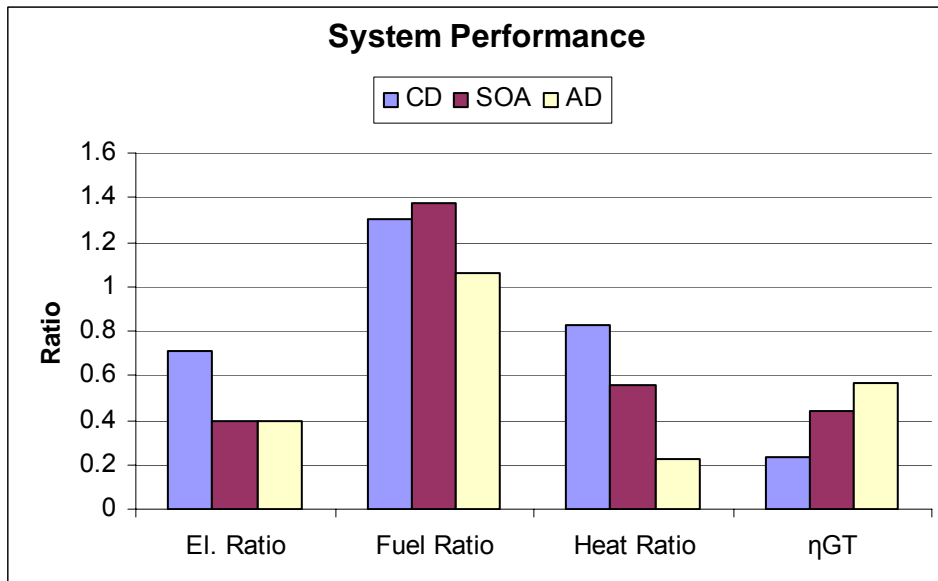
Figure 5.2: Main performance variables for the three main technological scenarios.

5.2   Electricity System Future Scenario

The main future electricity system development assumptions are based on the report "Inverstering og prisdannelse på et liberaliseret Elmarked" as described in Section 2.x (Morthorst et al.). The main value adopted from that report is the annual average electricity price. Values for the future natural gas and CO_2 quota price are based on the Danish Energy Authority future projections and are adopted unchanged in this analysis.

Values for system price sensitivity have been examined in (Lund et al., 2004). In this study, a value of 0.02 sensitivity is suggested for system prices of an average of 150 DKK/MWh. The higher the system price goes, the higher the sensitivity becomes. At prices of 500 DKK/MWh, a sensitivity of 0.1 is calculated based on the 2002-2003 values. The main electricity system assumptions are summarized in table 5.2.

	2010	**2015**	**2020**	**Unit**
El Price Average	200	250	400	[DKK/MWh]
ScaleUp	0	0	0	
ScaleDown	0	0	0	
DepFactorSupply	0.04	0.06	0.1	
DepFactorDemand	0.02	0.03	0.5	
CO2 Price	50	100	100	[DKK/Ton CO2]
Ngas Price	25.3	25.5	27.7	DKK/GJ
Ngas Price	91.08	91.8	99.72	DKK/MWh

Ngas Energy Content	39.6	39.6	39.6	MJ/m3
CO2 emission	0.057	0.057	0.057	[Ton CO2/GJ]
Total Ngas price including CO2	1,432	2,840	2,842	[DKK/GJ]
Total Ngas price including CO2	5,158	10,225	10,233	[DKK/MWh]

Table 5.2: Main electricity system variables used in the future scenario modeling.

5.3   Simulation Results

The electricity price time series used is the modified 2002 series described in section 2.3 In this series, 4 seasons for price variation can be readily distinguished as shown in Figure 5.3. Separate simulations are thus performed for each period, and the optimal bidding strategy and resulting variable operational cost (VAOI) are calculated as described in section 4.3. Since the series is "mirrored" about its half, results from periods IV and V are assumed to be the same as results from periods II and I respectively. The VAOI is then found by adding the operational costs of the 5 periods.
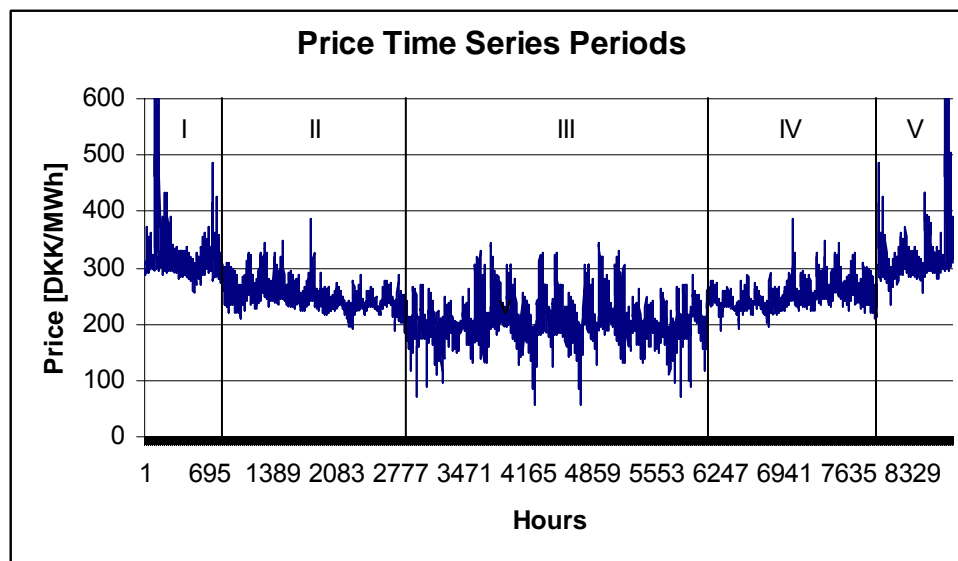
Figure 5.3: Simulation price period division based on seasonal changes in the price time series.

The results for the three technologies at 2 different storage sizes are shown in Figures 5.4 and 5.5 for the years 2010 and 2020. Both figures show that better technology results in higher VAOI. Besides, it is seen that the VAOI increases proportionally to the turbine capacity. This proportional relation was tested for several turbine capacities and found to confirm a linear relation very closely, so a linear relation was used to fill the

data points between the extreme turbine capacities in order to save simulation time. The figures also show that the VAOI for the year 2020 is significantly higher than that of 2010 for all three technologies.
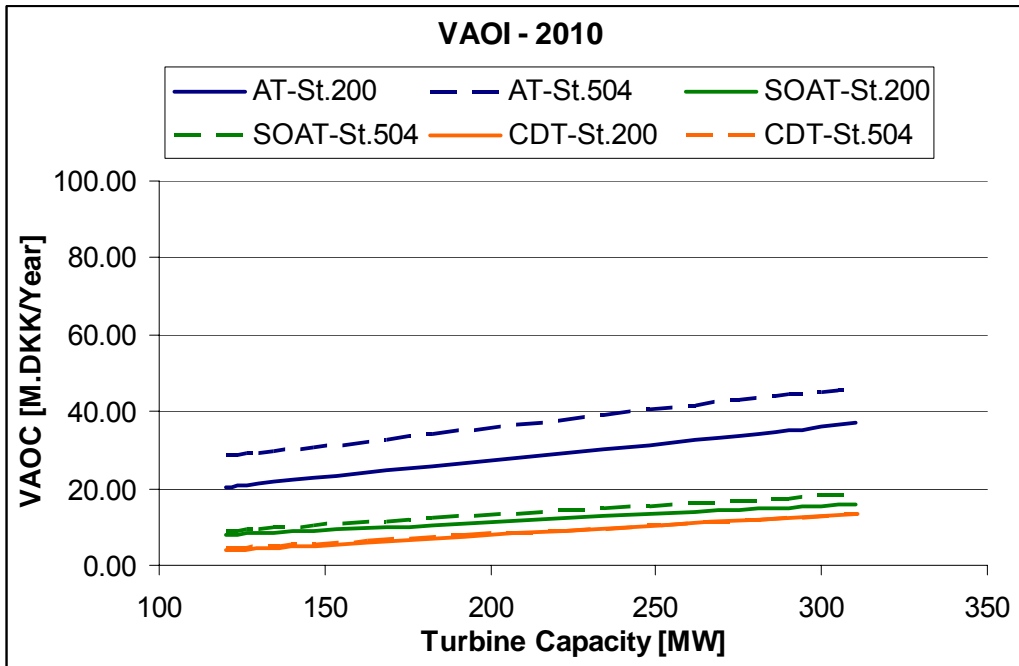
Figure 5.4: Variable Annual operational Cost (VAOI) for the year 2010 for various turbine capacities at cavern sizes of 200,000m^3 and 504,000m^3 respectively
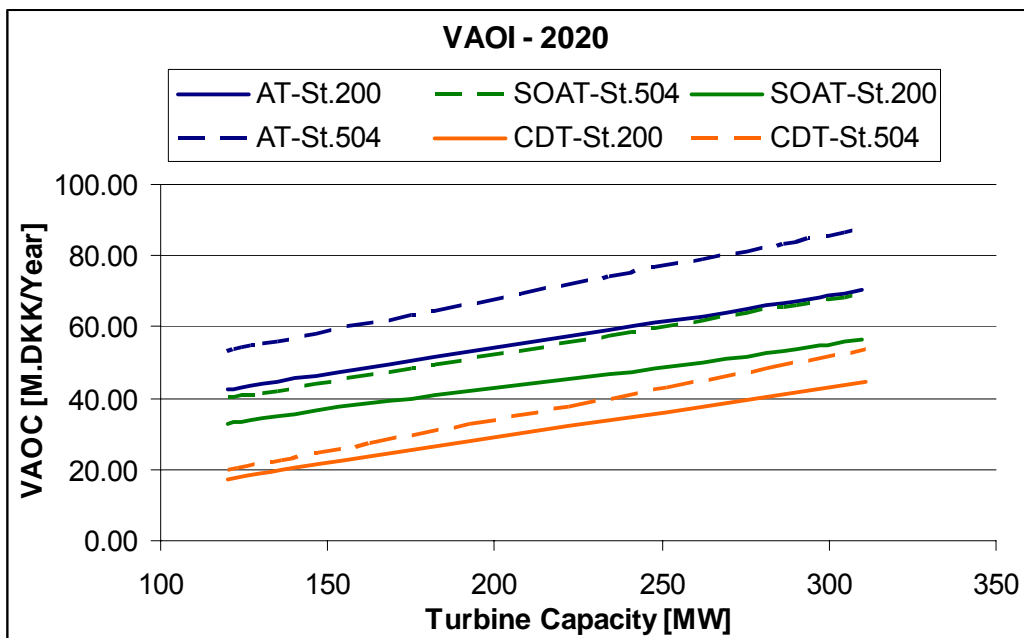
Figure 5.5: Variable Annual operational Cost (VAOI) for the year 2020 for various turbine capacities at cavern sizes of 200,000m^3 and 504,000m^3 respectively

Figure 5.6 shows the resulting annual turbine operational hours for the years 2010 and 2020 for the SOAT and the AT. The figures in the graph suggest that for a small storage size of 200,000m^3, the number of operational hours is barely changed between the years 2010 and 2020 for both technologies. For the larger storage however, the AT tends to operate a larger amount of hours in 2010. Figure 5.6 along with figures 5.4 and 5.5 can be used to understand the factors affecting the CAES plant operation, namely storage size, efficiency, and price fluctuations. In a least fluctuation scenario, efficiency and storage size act as a limiting factor to the possible amount of operation. As prices fluctuate more, the effect of efficiency is reduced, and the storage size becomes the dominant factor limiting the number of operational hours.
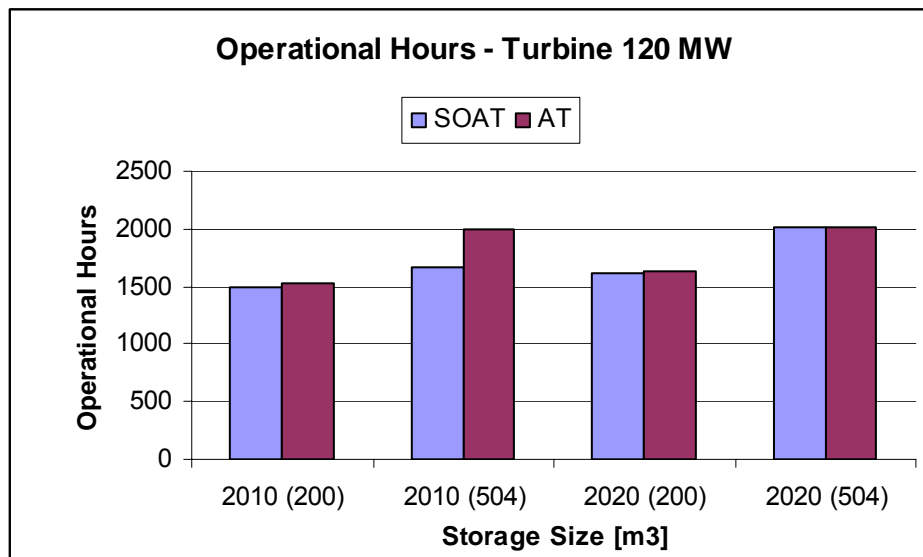
Figure 5.6: Number of turbine operational hours for a turbine capacity of 120 MW, storage sizes of 200,000m^3 and 504,000m^3, and years 2010 and 2020.

5.4   Feasibility Study

Table 5.3 summarizes the main investment costs, the fixed annual costs, and the key financial parameters used. The investment costs for the cavern are based on values from (Brix and Szameitat, 2003) whose values are based on correspondence with Dong. The equipment cost is based on the technology catalogue (ENS et al., 2005) where values in that report are given in terms of unit turbine capacity. In order to allow for the variation of the turbine size, certain ratios of are allocated to divide the reference source between the compression, expansion, and motor/generator sections of the plant. The technology

catalogue also reports values for fixed annual operation and maintenance costs (FAC) for plants production range between up to 300 MW to be around 11,000 Euro/MW/year. These values are compared to single cycle GT values of around 7000 Euro/MW/year for turbines up to 150 MW. It is assumed that future fixed CAES costs approach those for single cycle gas turbines, and the fixed costs are assumed to range between 10,000 Euro/MW/year to 4,000 Euro/MW/year. A rate of 7.5 is used to convert these prices to Danish Krone.

	CDT	SOAT	AT	Unit
Cavern [1]	321	321	321	DKK/m3
Investment/Generation Capacity [2]	2.7	2.7	2.7	M.DKK/MWh
Component Price Ratio				
Compressor+ Intercooler	0.30	0.30	0.30	-
Turb + Burner + Regenerator	0.50	0.50	0.50	-
Motor/Generator	0.20	0.20	0.20	-
Component Cost				
Compressor+ Intercooler	0.81	0.81	0.81	M.DKK/MW
Turb + Burner + Regenerator	1.35	1.35	1.35	M.DKK/MW
Motor/Generator	0.54	0.54	0.54	M.DKK/MW
Land/Building/Transactions	20	20	20	M.DKK
Heat Storage	0	0	1700	DKK/m3
Fixed Costs				
Fixed O&M Cost [50MW - 150MW]	75,000	75,000	75,000	DKK/MW/Year
Fixed O&M Cost [150MW - 250MW]	45,000	45,000	45,000	DKK/MW/Year
Fixed O&M Cost [>250MW]	30,000	30,000	30,000	DKK/MW/Year
Other Parameters				
Lifetime	30	30	30	Years
Interest Rate	4.00%	4.00%	4.00%	%

Table 5.3: Assumed investment costs, fixed annual costs and other financial parameters.

The total investment cost is calculated for each of the technical scenarios, and the results are divided to equal annual payments over the lifetime using the Net Present Value (NPV) relation:

$$NPV = \frac{AIC \times i}{(1 - (1+i)^{-n})} \quad \text{...................................5.1}$$

Where AIC is the annualized investment cost, i is the interest rate, and n is the lifetime. Using the above relation assumes no salvage value for the equipment and land after the investment. If a salvage value was included, the NPV of the investment can be first adjusted to accommodate for the salvage value at the given interest rate, and later equation 5.1 can be used to find the AIC.

The AIC and the fixed annual cost (FAC) are subtracted from the VAOI to find the net annual profit (NAP). Figures 5.7 through 5.9 show the graphs for the NAP for the three main technology scenarios consequently. The simulations are done for the years 2010-2015-2020, and a linear interpolation is used to connect values in between. The results shown are for extreme storage and turbine capacities simulated. Figure 5.7 shows that the CDT is not feasible for investment even at 2020 where prices fluctuations are large. As for the SOAT, a 120 MW turbine start being feasible around 2018, and the 310 MW turbine follows around 2020. Finally, the AT scenario is already feasible from 2012 for a 120 MW turbine, and a 310 MW follows around 2014.
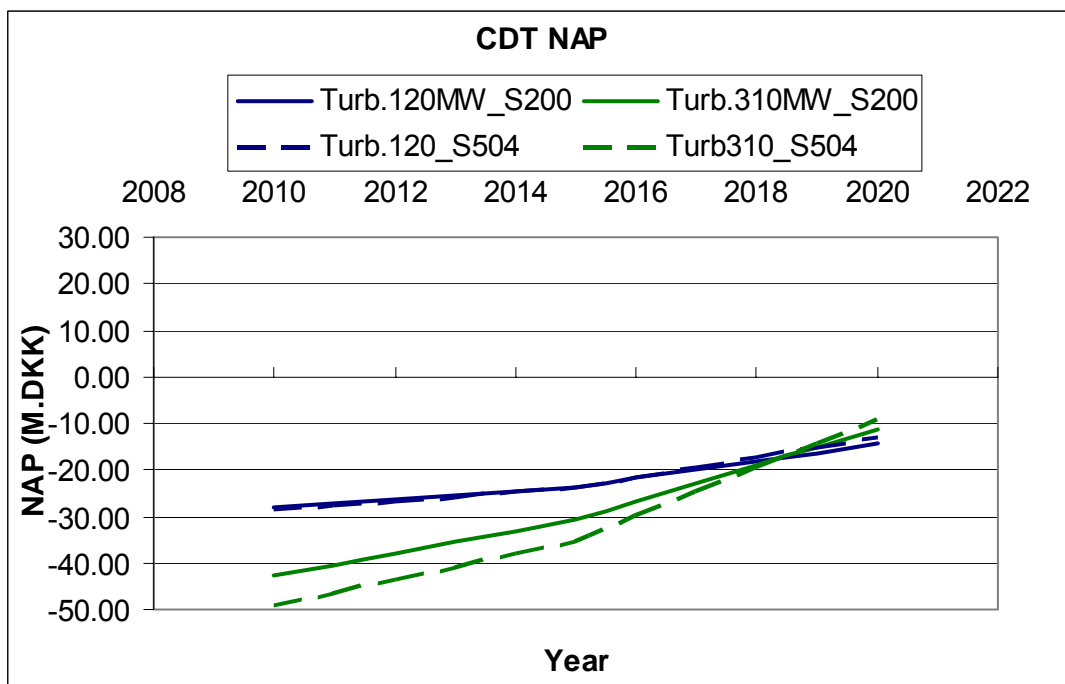
Figure 5.7: *the Net Annual Profit (NAP) for the Current Day Technology (CDT) for two values of storage size (200,000 m³ and 504,000 m³) and two turbine sizes (120 MW and 310 MW).*
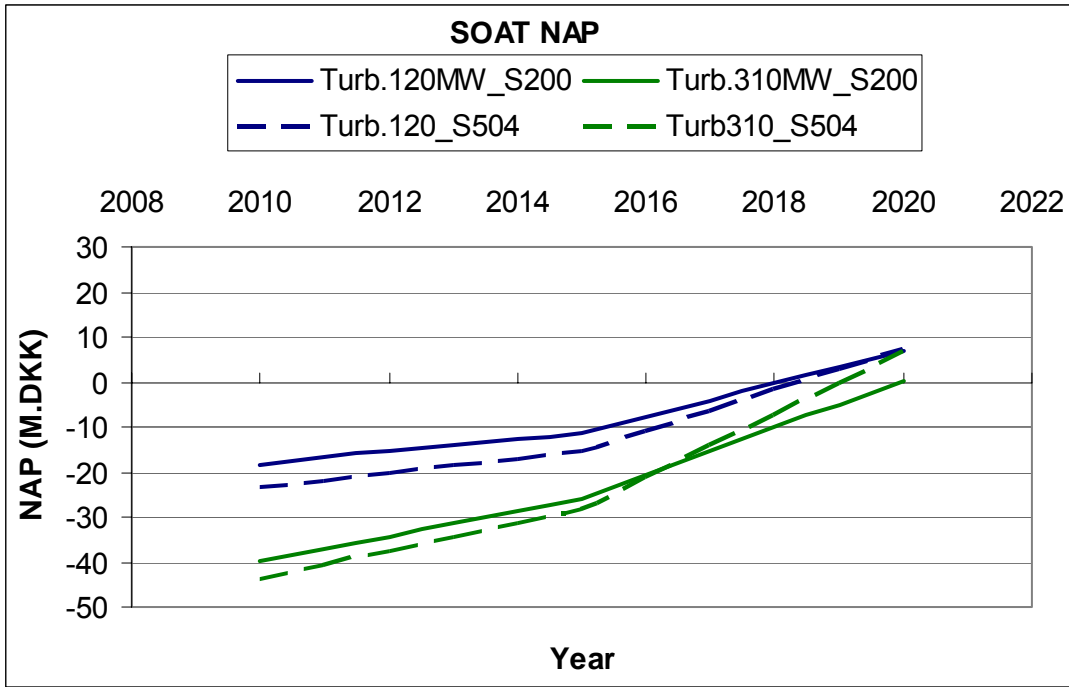
Figure 5.8: the Net Annual Profit (NAP) for the State of the Art Technology (SOAT) for two values of storage size (200,000 m^3 and 504,000 m^3) and two turbine sizes (120 MW and 310 MW).
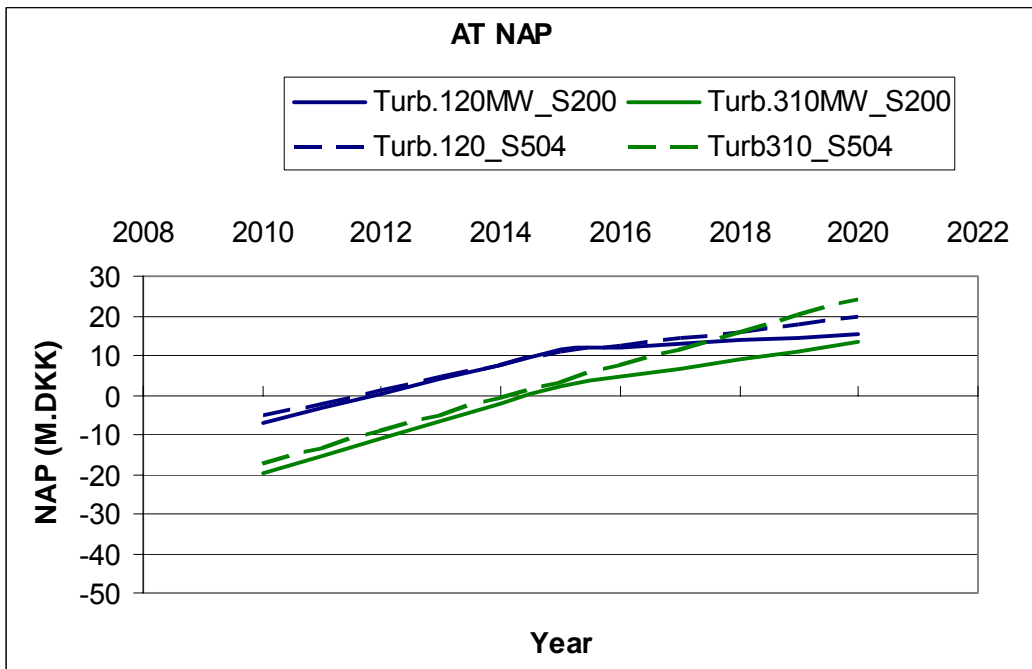
Figure 5.9: *the Net Annual Profit (NAP) for the Current Day Technology (CDT) for two values of storage size (200,000 m^3 and 504,000 m^3) and two turbine sizes (120 MW and 310 MW).*

Several comments regarding the plant dimensioning can be made based on Figures 5.9 through 5.9. During the initial years with low volatility, a smaller turbine capacity benefits from the lower investment cost and the higher efficiency to give a higher feasibility

than the 310 MW. However, as the fluctuation increases, larger turbine sizes start gaining significance and tend to exceed the profit from the small turbine. This is because as the price average increases, the time series displays sharper peaks. A 310 MW is better able to benefit from such peaks than a 120 MW turbines.

As the volatility increases also, the operational hours of the CDT and the SOAT increase. Besides having a better efficiency, a larger storage size gains advantage at high volatility as it allows for increased production hours with more freedom to locate these hours. As the years advance, storage size becomes a main deciding factor for the amount of production hours, which explains why the dashed lines exceed the solid lines in Figures 5.7 and 5.8 for advanced years. This is not the case for the AT, where storage size is already a limiting factor from the early years. This explains why dashed lines lie mainly above solid lines in Figure 5.9.

6. Conclusion and Reflections

A feasibility study for various technical and future prices scenario was performed. For this purpose, a technical model was developed that could simulate the behaviour of a CAES plant. This model is used within an operational model that optimizes the CAES plant operation.

It is found that improved CAES plant performance improve the feasibility of such a plant considerably. The plants improvements suggested in the technical scenarios involve higher firing temperatures for the turbine and heat storage for utilizing the compressor waste heat. Both technologies are readily available nowadays. Advanced technology plants can be feasible as early as 2012.

The recommended turbine capacity depends on the expected price average and fluctuation as well as the plant efficiency. At low price volatility, low turbine capacities are more feasible, whereas at higher price volatility, larger turbine capacities are more feasible. Concerning the storage size, larger storage sizes are favourable for advanced technology in all years and for state of the art technology in years with high price volatility. For the remaining cases, the number of operational hours is low so that the cavern size has little impact on the operation.

The value of the study performed is not in the exact financial numbers found. It is rather in identifying favourable technical and electricity system conditions that could make CAES as stated in the research question in Chapter 1. In this regard, the study has answered the question and identified scenarios of improved efficiencies and greater price volatility where CAES can be feasible.

Looking back at the research and the analysis, there are several points that would be interesting to include in a future study. The list below mentions some of the points that can be improved and further research in the future:

- Performing sensitivity analysis to variations in the assumed scenarios, in particular the price scenario. Dry years, wet years, and years with no wind are expected to significantly improve the CAES plant feasibility. Wet years and years with high wind levels are expected to have the opposite effect. It would be interesting to take a profile of 30 years that varies between the various weather conditions and examine the feasibility over that lifetime.

- Time did not allow for the simulation of operation on the regulating power market. It is expected that this would be a major source of profit for the CAES plant though, and such a simulation is desirable in the future.

- The system price reaction to the CAES production is modelled with a constant factor. It would be interesting to include a CAES plant in an overall energy model like SIVAEL or Balmorel and compare how could the exact system reaction to this new facility be.

- The price series is assumed to be deterministic. One very valuable simulation though would be to include the CAES plant in a stochastic model (such as Wilmar by Risø) where the real decision difficulty regarding the market and the prices to bid on can be studied.

- The overall environmental impact of a CAES plant can be further considered. One question is to know the main source of the electricity used for compression in order to better define the overall efficiency: Is the compressor operating at hours with lots of wind power, or is it not always the case? What are the CO_2 emissions saved both at the CAES plant and in terms of added wind power potential? Etc.

- CAES is considered to be a good alternative for dealing with the alternating wind power challenge. It could be interesting to compare CAES to other possible solutions such as heat pumps or hydrogen fuel cells, both in terms of feasibility and environmental impact.

- Natural gas is assumed to be the main fuel utilized at the plant. The availability of Natural gas in the lifetime of the project is very suspicious, in particular from local Danish production. Future studies should consider this factor and study other potential fuels like biogas or hydrogen combustion. This can improve the plant operation by avoiding the CO_2 quota price.

The above list can be expanded to include many other points. For now however, the study is concluded by stating that CAES investment can have a good investment potential in the future. The better the technological development, the less the dependency on higher price fluctuations for operation.

References

Boyce, 2002: Boyce M.P., <u>Handbook for Cogeneration and Combined Cycle Power Plants</u>, ASME Press, New York, 2002.

Brix and Szameitat, 2003: Brix W., Szameitat N., <u>CAES – Muligheder I Danmark</u>, Danish Technical University, Institute of mechanics, energy and construction., spring 2003.

Crotogino et al., 2001: Crotogino F., Mohmeyer K.U., Scharf R., <u>Huntorf CAES: More than 20 years of Successful Operation</u>, KBB GmbH and E.ON Kraftwerke Bremen, Spring 2001 Meeting, Orlando, Florida, USA, 15-18 April, 2001.

ENS et al., 2005: Energistyrelsen, Eltra, and Elkraft, <u>Technology Data for Electricity and Heat Generating Plants</u>, March 2005

ERDA, 1976: Energy Research and Development Administration, Compressed Air energy Storage, 1976.

Gresh, 2001: Gresh M.T., Compressor Performance: Aeorodynamics for the user 2nd edition, Butterworth-Heinemann, 2001.

LCRA, 2003: Lower Colorado River Authority, <u>Study of Electric Transmission in Conjunction with Energy Storage Technology</u>, Texas State Energy Conservation Office, August 21, 2003.

Lund et al., 2004: Lund H., Østergaard P.A., Andersen A.N., Hvelplund F., Mæng H., Munster E., Meyer N., <u>Lokale Energimarkeder</u>, Skriftseries nr 290, Institute for Social Development and Planning, Aalborg University, January 2004.

Matta et al., 2004: Matta R.K., Mercer C.D., Tuthill R.S., <u>Power Systems for the 21$^{\underline{st}}$ Century – "H" Gas Turbine Combined Cycles</u>, GE Power Systems, Schenectady NY, 2004.

Morthorst et al., 2005: Morthorst P.E., Jensen G.S., Meibom P., <u>Investering og pris-dannelse på et liberaliseret elmarked</u>, Risø Research Center, Roskilde, Denmark, May 2005.

Nakhamkin et al. 2004: Nakhamkin M, Wolk R.H., Linden S., Hall R., Patel M., <u>New Compressed Air Energy Storage Concept Improves the Profitability of Existing Simple Cycle, Wind Energy, and Landfill Power Plants</u>, ASME paper GT2004-54278, ASME Turbo Expo 2004, 14-17 June Vienna, Austria.

Nakhamkin et al. 2003: Nakhamkin M., Pelini R., Patel M., Humid Air Injection Power Augmentation Technology has Arrived, ASME paper GT2003 – 38977, ASME Turbo Expo 2003, 16 – 19 June, Atlanta, Georgia, USA.

Sonntag et al., 2003: Sonntag R.E., Borgnakke C., Van Waylen G.J., Fundamentals of Thermodynamics, sixth edition, Jon Wiley & Sons, Inc., 2003